Title: Comparative 'omics analyses differentiate *Mycobacterium tuberculosis* and *Mycobacterium bovis* and reveal distinct macrophage responses to infection with the human and bovine tubercle bacilli

Running title: Host specificity and pathogenic mycobacteria

Kerri M. Malone[1#], Kévin Rue-Albrecht[1,2,¥], David A. Magee[2], Kevin Conlon[1], Olga T. Schubert[3,¶], Nicolas C. Nalpas[2§], John A. Browne[2], Alicia Smyth[1], Eamonn Gormley[4], Ruedi Aebersold[3,5], David E. MacHugh[2,6] Stephen V. Gordon[1,6,7,8,#]

[1]UCD School of Veterinary Medicine, University College Dublin, Belfield, Dublin 4, Ireland

[2]Animal Genomics Laboratory, UCD School of Agriculture and Food Science, University College Dublin, Belfield, Dublin 4, Ireland

[3]Department of Biology, Institute of Molecular Systems Biology, ETH Zurich, CH-8093, Switzerland

[4]Tuberculosis Diagnostics and Immunology Research Centre, UCD School of Veterinary Medicine, University College Dublin, Belfield, Dublin 4, Ireland

[5]Faculty of Science, University of Zurich, Zurich, Switzerland

[6]UCD Conway Institute of Biomolecular and Biomedical Research, University College Dublin, Belfield, Dublin 4, Ireland

[7]UCD School of Medicine, University College Dublin, Dublin 4, Ireland

[8]UCD School of Biomolecular and Biomedical Science, University College Dublin, Dublin 4, Ireland

Current address: [¥]Kennedy Institute of Rheumatology, Nuffield Department of Orthopaedics, Rheumatology and Musculoskeletal Sciences, University of Oxford, Headington, Oxford OX3 7FY, UK; [¶]Department of Human Genetics, University of California, Los Angeles, USA; [§]Quantitative Proteomics and Proteome Centre Tübingen, Interfaculty Institute for Cell Biology, University of Tübingen, Tübingen, 72076, Germany

[#]Correspondence: Kerri M. Malone, Email: kerri.malone@ucdconnect.ie; Stephen V. Gordon, Email: stephen.gordon@ucd.ie

Abstract word count: 226/250

Main text word count: 4,747/5,000

Abstract:

Members of the *Mycobacterium tuberculosis* complex (MTBC) are the causative agents of tuberculosis in a range of mammals, including humans. A key feature of MTBC pathogens is their high degree of genetic identity, yet distinct host tropism. Notably, while *Mycobacterium bovis* is highly virulent and pathogenic for cattle, the human pathogen *M. tuberculosis* is attenuated in cattle. Previous research also suggests that host preference amongst MTBC members has a basis in host innate immune responses. To explore MTBC host tropism, we present in-depth profiling of the MTBC reference strains *M. bovis* AF2122/97 and *M. tuberculosis* H37Rv at both the global transcriptional and translational level via RNA-sequencing and SWATH mass spectrometry. Furthermore, a bovine alveolar macrophage infection time course model was employed to investigate the shared and divergent host transcriptomic response to infection with *M. tuberculosis* or *M. bovis*. Significant differential expression of virulence-associated pathways between the two bacilli was revealed, including the ESX-1 secretion system. A divergent transcriptional response was observed between *M. tuberculosis* and *M. bovis* infection of bovine alveolar macrophages, in particular cytosolic DNA-sensing pathways at 48 hours post-infection, and highlights a distinct engagement of *M. bovis* with the bovine innate immune system. The work presented here therefore provides a basis for the identification of host innate immune mechanisms subverted by virulent host-adapted mycobacteria to promote their survival during the early stages of infection.

Importance:

The *Mycobacterium tuberculosis* complex (MTBC) includes the most important global pathogens for humans and animals, namely *Mycobacterium tuberculosis* and *Mycobacterium bovis*, respectively. These two exemplar mycobacterial pathogens share a high degree of genetic identity, but the molecular basis for their distinct host preference is unknown. In this work we integrated transcriptomic and proteomic analyses of the pathogens to elucidate global quantitative differences between them at the mRNA and protein level. We then integrated this data with transcriptome analysis of the bovine macrophage response to infection with either pathogen. Increased expression of the ESX-1 virulence system in *M. bovis* appeared a key driver of an increased cytosolic nucleic acid sensing and interferon response in bovine macrophages infected with *M. bovis* compared to *M. tuberculosis*. Our work demonstrates the specificity of host-pathogen interaction and how the subtle interplay between mycobacterial phenotype and host response may underpin host specificity amongst MTBC members.

Keywords: *Mycobacterium tuberculosis, Mycobacterium bovis*, cattle, gene expression, RNA-sequencing, SWATH mass spectrometry, transcriptomics, proteomics, host specificity, host-pathogen interactions, MTBC, infectious disease

Introduction

The *Mycobacterium tuberculosis* complex (MTBC) comprises ten mycobacterial species that cause tuberculosis (TB) in a broad range of mammalian species, including humans (1-4). Typically, MTBC species show greater than 99% nucleotide sequence identity and yet exhibit distinct host preference, indicating that this low-level of genetic divergence holds major implications for host-pathogen interactions (1-3). Divergence in host tropism is illustrated through the comparison of the human adapted *Mycobacterium tuberculosis* with the animal bacillus *Mycobacterium bovis*. *M. tuberculosis* is a highly successful pathogen and is the world's leading cause of death from an infectious agent with 1.7 million deaths reported in 2016 (5). *M. bovis* predominantly causes disease in cattle and bovine TB exacts a tremendous economic burden through production loss and control costs (6-8). *M. tuberculosis* appears unable to sustain (i.e., through cycles of infection, disease and transmission) in non-human animal populations, a fact that has been confirmed using an experimental bovine infection model (1, 9): while cattle infected with *M. bovis* display characteristic pathology, cattle infected with *M. tuberculosis* show minimal pathology despite positive skin-test and interferon-gamma responses indicative of successful infection. Conversely, while *M. bovis* can both infect humans and cause pulmonary disease that is clinically indistinguishable from *M. tuberculosis*, it rarely transmits among immunocompetent hosts (10, 11).

104 On a cellular level, the alveolar macrophage is the frontline host immune cell that
105 encounters both *M. tuberculosis* and *M. bovis,* and its role during early stage infection is
106 well established (12-18). Several studies have highlighted significant differences in the
107 production of key innate factors, chemokines and cytokines at both the transcript and
108 protein level in macrophages infected with *M. tuberculosis* or *M. bovis* (15-20).
109 However, these studies evaluated only a subset of the innate response in macrophages
110 and differences in the global transcript and protein response to infection with
111 *M. tuberculosis* or *M. bovis* remains unknown. The central role of the alveolar
112 macrophage during infection is also reflected in the fact that pathogenic mycobacteria
113 have evolved several immune-evasion strategies to circumvent the killing mechanisms
114 of the macrophage, including inhibition of phagosomal maturation, phagosomal escape
115 and suppression of innate immune signalling (12-18). This facilitates the dissemination
116 of the bacilli to other macrophages and ultimately throughout the host, with the
117 concomitant development of immunopathology. Transmission of infection then occurs
118 through the rupture of lesions into associated airways and the dispersal of bacilli
119 (17,18). Thus, it can be hypothesized that the initial interaction between host and
120 pathogen may be key for the host preference observed between *M. tuberculosis* and *M.*
121 *bovis*; whether this interaction has roots in host-centric or pathogen-centric processes,
122 or indeed a combination of both, has yet to be fully elucidated.

123 *M. tuberculosis* H37Rv and *M. bovis* AF2122/97 were the first MTBC genomes to
124 be fully sequenced and they represent the default reference strains for the human and
125 animal tubercle bacilli (2, 21, 22). It is hypothesized that host tropism between these

two species may be explained by differential gene expression profiles as a result of low genetic divergence (2, 21, 22). So far, functional studies have revealed that genetic changes between the two pathogens are responsible for differential nitrate reductase activity, for the loss of phenolic glycolipid production in *M. tuberculosis* H37Rv in contrast to *M. bovis,* and for differences in the PhoPR regulation system that governs the expression of virulence-related pathways such as EsxA/ESAT-6 secretion and cell wall lipid biosynthesis (23-26). While these studies highlight important differences between the two pathogens, host tropism likely involves a combination of events such as these that affect the expression and regulation of multiple virulence associated factors and/or the transcriptional regulators that govern their activity. In 2007, two microarray-based studies highlighted genes encoding the major antigens MPT83 and MPT70 that were expressed at higher levels in *M. bovis* and genes involved in SL-1 production that were expressed at a higher level in *M. tuberculosis* (27, 28). Since these reports, investigations into species-specific expression profiles of the two pathogens have been lacking at the global transcriptional level and have yet to be defined at the proteomic level. Definition of the differential "expressome" between *M. tuberculosis* and *M. bovis* will shed light on how alternate expression of two highly related genomes impacts on the ultimate success of these pathogens and host specificity within the MTBC.

As a route to defining host preference between *M. tuberculosis* and *M. bovis*, we have conducted in-depth profiling of *M. bovis* AF2122/97 and *M. tuberculosis* H37Rv at

148 both the global transcriptional and translational level *in vitro* using RNA-seq and
149 Sequential Window Acquisition of all Theoretical Spectra (SWATH) mass spectrometry, a
150 massively parallel targeting mass spectrometry that provides highly reproducible
151 quantitative measurements across samples (29). To address how MTBC pathogen
152 variation impacts on the host innate response, we have performed detailed comparative
153 transcriptomic analyses of the bovine alveolar macrophage response to infection with
154 both pathogens using RNA-sequencing (RNA-seq). Through these analyses, we reveal
155 significant differential expression of virulence-associated pathways between *M.*
156 *tuberculosis* and *M. bovis* was found, in particular the ESX-1 secretion system, while the
157 macrophage infection study highlights a distinct engagement of *M. bovis* with the
158 bovine innate immune system was found, in particular with the cytosolic DNA-sensing
159 pathways of the macrophage.

160

Methods

Mycobacterial culture for pathogen transcriptomics and proteomics

Exponentially grown mycobacterial liquid cultures were established in Sauton's basal media +0.025% tyloxapol. For mid to late-log phase culture, mycobacterial cells were grown to an optical density (OD_{600nm}) of 0.6 – 0.8 at 37^{o}C prior to harvest. For the current study, six *M. bovis* AF2122/97 and six *M. tuberculosis* H37Rv replicates were prepared. Matched RNA and protein samples were harvested and prepared for strand-specific RNA-sequencing or SWATH mass spectrometry.

RNA extraction, RNA-seq library preparation and high-throughput sequencing for *M. bovis* and *M. tuberculosis*

Mycobacterial cells were harvested by centrifugation at 2,500 × g for 10 min and the pellet was re-suspended in 1 ml of TRIzol® (Life Technologies). The suspension was transferred to a 2 ml screw cap tube and the cells were lysed by bead-beating for 30 s at maximum setting using 1 mm glass beads (Sigma) on a MagNaWLyser instrument (Roche). Samples were placed at 80^{o}C immediately and thawed before use. 20% v/v chloroform was added, the sample were shaken vigorously for 15 s and incubated for 2-3 min at room temperature. The samples were centrifuged at 12,000 × g for 15 min at 4°C and the top phase was added to the DNA-free columns from the RNeasy plus kit (Qiagen). The sample were processed as per the manufacturer's guidelines with the following exceptions: 1.5 volumes of 100% ethanol was added to sample prior to its application to the RNeasy column in order to recover all RNA species. RNA was eluted in

molecular grade water and its concentration was determined using the NanoDrop spectrophotometer (NDW1000) prior to DNase treatment. A DNase treatment using TURBO DNase kit (Thermo Fisher Scientific) was performed by following the vigorous DNase treatment as per manufacturer's guidelines; 7 µl of DNase buffer + 1 µl enzyme at 37°C for 30 min followed by a further 1 µl of enzyme and incubation at 37°C for 30 min. A DNase stopping solution was not added to the samples as they were column-purified and concentrated using the RNA Clean and Concentrator kit according to manufacturer's guidelines (Zymo). RNA was eluted in molecular grade water and its concentration was determined using the NanoDrop spectrophotometer (NDW1000). RNA integrity number (RIN) values were assessed for each RNA sample being considered for RNA-sequencing using the 2100 Bioanalyser (Agilent) and the RNA 6000 Nano kit (Agilent) according to manufacturer's guidelines. RIN values are calculated by assessing the entire electrophoretic trace of an RNA sample, along with the 23S/16S rRNA intensity value. Only samples with a RIN value > 8 were selected for further analysis by RNA-sequencing. Sequencing libraries were prepared at the Genomics Core, Michigan State University, Michigan, USA using the Illumina Truseq Stranded Total RNA Library Prep Kit LT and the Epicenter RiboWZero Magnetic Bacteria kit to deplete ribosomal RNA. Single-end, strand-specific 50 bp read data was produced with base calling performed by Illumina Real Time Analysis (RTA) v1.18.64.

Differential gene expression analysis of *M. bovis* and *M. tuberculosis* RNA-sequencing data

Computational analyses were performed on a 32-node Compute Server with Linux

Ubuntu [version 12.04.2]. Briefly, adapter sequence contamination and paired-end reads of poor quality were removed from the raw data. At each step, read quality was assessed with FastQC [version 0.10.1] (30). Single-end reads were aligned to the *M. bovis* AF2122/97 or *M. tuberculosis* H37Rv reference genomes with the aligner Stampy in hybrid mode with BWA (31). Read counts for each gene were calculated using featureCounts, set to unambiguously assign uniquely aligned single-end reads in a stranded manner to gene exon annotation (32).

Prior to cross-species differential expression analysis, an Identical/Variable gene dataset was constructed for *M. tuberculosis* H37Rv and *M. bovis* AF2122/97 where orthologous genes were separated into those genes whose protein products are of equal length and 100% conserved at the amino acid level (Identical, *n* = 2,775) from those that are not (Variable, *n* = 1,224). (Fig.1A, Supp_I.xlsx). Among the Variable genes are examples of truncated genes, genes that have been split into two or more as a result of in-frame sequence variance (leading to some genes being represented in more than one Variable gene pair), or genes that differ by a non-synonymous SNP resulting in an amino acid change at the protein level. Negative binomial modelling tools such as DESeq2 that was used in this instance assume equal feature lengths when calculating differential expression (DE) of a gene, or in this case between orthologous genes of two species in a given condition (33). For those annotations whose gene lengths are not equal, such as in the case of truncated/elongated/frameshift instances found in the *M. bovis* AF2122/97 genome with respect to *M. tuberculosis* H37Rv, analysis with DESeq2 would result in erroneous differential expression results; thus a separate differential

226 expression analyses was carried out for Variable genes using Transcript per Million
227 (TPM) values that are normalised for feature length (33, 34). Differential gene
228 expression analysis for those genes of equal lengths was performed using the DESeq2
229 pipeline, correcting for multiple testing using the Benjamini-Hochberg method (33). All
230 further reference to differentially expressed genes between the two mycobacterial
231 species will be with regards to a gene being expressed at a higher level in one species
232 with respect to the other, and hence if a gene is upregulated in *M. bovis* it is
233 downregulated or expressed at a lower level in *M. tuberculosis* and vice versa ($\log_2$ fold
234 change ($Log_2FC > 1$ and < -1), false discovery rate (FDR) threshold of significance < 0.05).

235 **Transcription factor enrichment analysis**

236 Data relating to the shift in the transcriptional landscape of *M. tuberculosis* upon
237 overexpression of 183 transcription factors was used to perform a formal transcription
238 factor enrichment analysis (35-37). The data represents 9,335 regulatory events and
239 provides regulatory evidence for over 70% of the annotated genes in the *M. tuberculosis*
240 genome ($FC > 2$, $P < 0.01$) (35-37). This data was analysed alongside the DE genes
241 identified in this study between *M. bovis* and *M. tuberculosis*. Only genes and
242 transcription factors that are 100% identical in sequence and length between the two
243 species were considered for this analysis. Over-representation of a transcription factor
244 with a given set of differentially expressed genes was assessed by gene-regulon
245 association and calculation of the Rand Index ($Log_2FC > 1$ and $P < 0.05$ for a given DE
246 gene).

247

248 **Protein extraction and SWATH mass spectrometry for *M. bovis* and *M. tuberculosis***

249 Mycobacterial cells were harvested by centrifugation at 2,500 × g for 10 min and the
250 pellet was re-suspended in 1 ml LB buffer (0.1 M ammonium bicarbonate buffer, 8 M
251 urea, 0.1% *Rapi*GEST SF (Waters, UK)). The suspension was transferred to a 2-ml screw
252 cap tube and the cells were lysed by bead-beating for 30 s at maximum setting using 3
253 mm glass beads (Sigma) and a MagNaLyser instrument (Roche). The lysate supernatant
254 was harvested by centrifugation at 12,000 × *g* for 10 min and transferred to a clean 1 ml
255 tube. The remaining pellet was re-suspended in LB buffer and the bead beating cycle
256 was repeated twice more. Protein lysate samples were stored at -80°C. Protein samples
257 were removed from -80°C storage and thawed on ice. Total protein content was
258 measured using the Qubit Protein Assay kit according to manufacturer's guidelines and
259 protein concentrations were adjusted to 0.5 mg/ml. Protein disulphide bonds were
260 reduced by addition of 0.2 M Tris(2-carboxyethyl)phosphine (TCEP) and the resulting
261 free cysteine residues were alkylated by addition of 0.4 M iodoacetamide (IAA).
262 Extracted protein samples were diluted with 0.1 M ammonium bicarbonate buffer to
263 reach a urea concentration of < 2 M and then digested with 1:50 enzyme/substrate ratio
264 of sequencing grade modified trypsin (Promega). 50% trifluoroaceticacid (TFA) was
265 added to lower the pH to 2 in order to stop the tryptic digest and to precipitate the
266 *Rapi*GEST. Water-immiscible degradation products of *Rapi*GEST were pelleted by
267 centrifugation at 12,000 × *g* for 10 min. The cleared peptide solution was desalted with
268 C18 reversed-phase columns (SepWPak Vac C18, Waters). The columns were pre-

conditioned 2-3 times with acetonitrile and equilibrated 3 times with Buffer A (2% acetonitrile, 0.1% trifluoroacetic acid in H_2O) prior to sample loading. The flow-through was re-loaded onto the column and the column was then washed 3 times with Buffer A. The peptides were eluted from the column using Buffer B (50% acetonitrile, 0.1% trifluoroacetic acid in H_2O) and the elution step was repeated. The eluate was dried under vacuum using a rotary evaporator at 45°C. Dried peptide pellets were re-suspended in MS buffer (2% acetonitrile, 0.1% trifluoroacetic acid in ultra pure H_2O) to a concentration of 1 µg/µl, sonicated in a water bath for 3 min and supernatant was harvested by centrifugation at 12,000 × *g* for 10 min.

SWATH mass spectrometry measurements were conducted at the Institute for Molecular Systems Biology at ETH Zurich. 1 µg of each peptide sample was measured in SWATH mode on a TripleTOF 5600 mass spectrometer using data-independent acquisition settings as described earlier (29, 38-40). Resulting raw SWATH data was analysed using an automated pipeline and the software OpenSWATH with the *M. tuberculosis* H37Rv SWATH assay library (38). Differential expression analysis of protein identified in *M. tuberculosis* and *M. bovis* samples was dependent on the detection of the protein in both species. The difference in protein fold changes and the corresponding FDR corrections between *M. tuberculosis* and *M. bovis* were calculated using MSstats (39, 41). A $|Log_2FC| > 0.56$ and an FDR < 0.05 was required for a protein to defined as differentially expressed between *M. tuberculosis* and *M. bovis.*

Animals

All animal procedures were performed according to the provisions of the Irish Cruelty to Animals Act of 1876 with ethical approval from the University College Dublin (UCD) Animal Ethics Committee (protocol number AREC-13-14-Gordon). Ten unrelated Holstein-Friesian male calves (7-12 weeks old) were maintained under uniform housing conditions and nutritional regimens at the UCD Lyons Research Farm (Newcastle, County Kildare, Ireland). All animals were selected from a tuberculosis-free herd that is screened annually using the single intradermal comparative tuberculin skin test.

Alveolar macrophage isolation, cell culture and infection

The laboratory methods used to: (1) isolate, culture and infect bovine alveolar macrophages with *M. bovis* and *M. tuberculosis*, and (2) generate strand-specific RNA-seq libraries using RNA harvested from these cells has been described in detail by us elsewhere (15, 42). An abridged description of the laboratory methods used in this study is provided below and the complete bioinformatics pipeline is accessible online (https://github.com/kerrimalone/AlvMac). Total lung cells were harvested by pulmonary lavage of lungs obtained post-mortem and stored in freezing solution (10% DMSO (Sigma-Aldrich Ltd.), 90% FBS) at a density of 2.5×10^7 cells/ml in 1 ml cell aliquots at −140°C. When required, the cell pellet was resuspended in 15 ml of $R10^+$ media and placed in a 75 cm^2 vented culture flask (CELLSTAR®, Greiner Bio-One Ltd.) and incubated for 24 h at 37°C, 5 % CO_2. After incubation, media was removed together with non-adherent cells, adherent cells were washed with 15 ml HBSS pre-warmed to 37°C and dissociated by adding 10 ml pre-warmed 1× non-enzymatic cell dissociation solution (Sigma-Aldrich Ltd.) to each culture flask. Cells were then pelleted (200 × g for 5

min), resuspended in 10 ml pre-warmed R10+ media and counted using a Vi-CELL™ XR Cell Viability Analyzer and reagent kit (Beckman Coulter Inc.). Mean viable cell recovery was estimated at ~ 80% for each animal. Cell counts for each animal were adjusted to 5×10^5 cells/ml (based on viable cell counts) using pre-warmed R10+ media, seeded at 5×10^5 cells/well on individual 24-flat well tissue culture plates (Sarstedt Ltd.) and incubated for a further 24 h at 37°C, 5 % CO_2, until required for mycobacterial infection. The purity of the seeded macrophages for each animal samples was 95% as estimated by flow cytometry analysis (data not shown).

M. bovis AF2122/97 and *M. tuberculosis* H37Rv were cultured in Middlebrook 7H9-ADC medium containing either 0.2% v/v glycerol for *M. tuberculosis* or 10 mM sodium pyruvate for *M. bovis* at 37°C until mid-logarithmic phase. Prior to infection, mycobacterial cultures were pelleted by centrifugation (200 × g, 10 min), pellets were disrupted with 3 mm sterile glass beads (Sigma-Aldrich Ltd.) by vortexing at top speed, 1 min. Cells were resuspended in pre-warmed R10 media, sonicated at full power (Branson Ultrasonics Corporation) for 1 min and the cell number was then adjusted to 5×10^6 bacterial cells/ml (OD_{600nm} of 0.1 = 1×10^7 bacterial cells) for a multiplicity of infection (MOI) of 10 bacilli per alveolar macrophage.

For the infection time course, the R10 media was removed from the macrophages and replaced with 1 ml R10 media containing *M. bovis* or *M. tuberculosis* (5×10^6 bacilli/ml); parallel non-infected control alveolar macrophages received 1 ml R10 media only. The alveolar macrophages were incubated at 37°C, 5 % CO_2 for times of 2, 6, 24

and 48 hours post-infection (hpi). Following completion of the 2 hpi time point, the 2 hpi macrophages were lysed (by adding 250 µl RLT-1% β-mercaptoethanol buffer per tissue culture plate well) and stored at −80°C, while the media for the 6, 24 and 48 hpi macrophages was replaced with 1 ml fresh R10 media per well and cells were reincubated at 37°C, 5 % CO_2 until required for harvesting. CFU were monitored over the infection time course (Fig.S1).

RNA extraction, RNA-seq library preparation and high-throughput sequencing for bovine alveolar macrophage samples

For the current study, 117 strand-specific RNA-seq libraries were prepared. These comprised *M. bovis*-, *M. tuberculosis*- and non-infected samples from each time point (0, 2, 6, 24 and 48 h) across 10 animals (with the exception of one animal that did not yield sufficient alveolar macrophages for *in vitro* infection at the 48 hpi time point). RNA extractions from macrophage lysates included an on-column genomic DNA elimination step (RNeasy® Plus Mini kit (Qiagen Ltd)). RNA quantity and quality was assessed using a NanoDrop™ 1000 spectrophotometer (Thermo Fisher Scientific Inc.) and a Bioanalyzer and an RNA 6000 Nano LabChip kit (Agilent Technologies Ltd). All samples displayed 260/280 ratio > 2.0 and RNA integrity numbers > 8.5. 200 ng total RNA from each sample was used for RNA-seq library preparation. Poly(A) mRNA enrichment was performed (Dynabeads® mRNA DIRECT™ Purification Kit (Invitrogen, Life Technologies)) and Poly(A)-enriched mRNA was used to prepared individually barcoded strand-specific RNA-seq libraries (ScriptSeq™ version 2 RNA-Seq Library Preparation Kit (Illumina, San Diego, CA, USA)). The libraries were pooled into three sequencing pools and sequenced

355 across 24 flow cell lanes (Illumina® HiSeq2000, Beijing Genomics Institute, Shenzhen,
356 China).

357 **Differential gene expression analysis of bovine alveolar macrophage RNA-sequencing**
358 **data**

359 Computational analyses was performed on a 32-node Compute Server with Linux
360 Ubuntu [version 12.04.2]. Briefly, pooled libraries were deconvoluted, adapter sequence
361 contamination and paired-end reads of poor quality were removed. At each step, read
362 quality was assessed with FastQC [version 0.10.1] (30). Paired-end reads were aligned to
363 the *Bos taurus* reference genome (*B. taurus* UMD3.1.1) with STAR aligner (43). Read
364 counts for each gene were calculated using featureCounts, set to unambiguously assign
365 uniquely aligned paired-end reads in a stranded manner to gene exon annotation (32).
366 Differential gene expression analysis was performed using the edgeR Bioconductor
367 package that was customized to filter out all bovine rRNA genes, genes displaying
368 expression levels below one count per million [CPM] in at least ten individual libraries
369 and identify differentially expressed (DE) genes between all pairs of infection groups
370 within each time point, correcting for multiple testing using the Benjamini-Hochberg
371 method with $Log_2FC > 1$ and < -1 and an FDR threshold of significance < 0.05 (44, 45).
372 Cellular functions and pathways over-represented in DE gene lists were assessed using
373 the SIGORA R package (46).

374 **Data availability**

375 RNA-seq datasets can be found using accession number PRJEB23469. SWATH MS data
376 and OpenSWATH outputs can be found on PeptideAtlas under identifier PASS00685
377 (http://www.peptideatlas.org/PASS/PASS00685).
378
379

Results

Differential RNA and protein expression between *M. bovis* and *M. tuberculosis*

For this study, 12 strand-specific RNA-seq libraries were prepared from *M. bovis* AF2122/97 (*n* = 6) and *M. tuberculosis* H37Rv (*n* = 6) grown exponentially in Sauton's basal media pH 7.0 (Fig.S2; mapping statistics can be found in Supp_II.csv). An 'Identical'/'Variable' gene dataset was constructed where orthologous genes between the two species were separated into those genes whose protein products are of equal length and 100% conserved at the amino acid level (Identical, *n* = 2,775) from those that are not (Variable, *n* = 1,224). (Fig.1A, Supp_I.xlsx). 170 and 146 differentially expressed (DE) Identical genes and 133 and 124 DE Variable genes were identified for *M. bovis* and *M. tuberculosis* respectively, amounting to 573 DE genes in total (Fig.1A, B, Supp_III.xlsx). Twelve SWATH mass spectrometry (MS) datasets were generated from total protein samples harvested from the same cultures as the RNA (Fig.S2, Fig.S4, Supp_III.xlsx). Overall, 2,627 proteins were detected using the *M. tuberculosis* assay library (~70% and ~56% of total Identical and Variable protein, respectively) (Fig.S4, Supp_III.xlsx) (38, 40). Of the 1,937 Identical proteins detected by SWATH MS, 232 and 218 proteins were found to be upregulated *M. bovis* and *M. tuberculosis* respectively, totalling 450 DE proteins (Fig.1A, B, Supp_III.xlsx). 133 and 215 Variable proteins were found to be upregulated *M. bovis* and *M. tuberculosis* respectively, amounting to 348 DE Variable proteins in total (50.4%) (Fig.1A, B, Supp_III.xlsx). Overlap of the DE lists for *M. bovis* and *M. tuberculosis* revealed 77 and 103 genes that are significantly upregulated

401 in either species at both the RNA and protein level respectively (Fig.1D); the top 20 of
402 these are represented in Fig.1C.

403 Genes encoding Mpt70 and Mpt83 are the top two genes upregulated at the RNA
404 and protein level in *M. bovis*; this is a result of a non-operational anti-SigK protein in *M.*
405 *bovis* leading to constitutive upregulation of the SigK regulon, of which the *mpt83* and
406 *mpt70* genes are components (47). Furthermore, Rv0216/Mb0222, a double hotdog
407 hydratase, is upregulated in *M. bovis* at both the RNA and protein level as previously
408 observed by microarray analysis (27). Amongst the genes upregulated at both the RNA
409 and protein level in *M. tuberculosis* H37Rv are: *ppe51*; antitoxin *vapB47*; and nitrate
410 reductase associated genes *narH* and *narG,* previously reported as upregulated at the
411 RNA level in *M. tuberculosis* in comparison to *M. bovis* as a result of a SNP in the
412 promoter region of *narGHJI* (Fig.1C)(25, 26). Incomplete overlap between DE genes at
413 the transcriptional and translational level seen in this study has been reported in other
414 studies and can be attributed to post-transcriptional and post-translational regulation
415 within the cell, but also to more technical aspects, such as differences in detection limits
416 and particular thresholds chosen to define differentially expressed RNA or protein (48-
417 50).

418

419 **Transcription factor enrichment analysis: the PhoP regulon and ESX-1 secretion system**

420 The differential gene expression observed between *M. bovis* and *M. tuberculosis*
421 may be a consequence of differences in global transcriptional network regulation

between the two species. To address this hypothesis, a formal transcription factor enrichment analysis was performed and revealed the significant association of 16 transcription factors with the DE Identical genes between *M. bovis* (*n* = 146) and *M. tuberculosis* (*n* = 170) (Fig.1E) (37). The association of transcription factors such as alternate sigma factors SigK and SigF along with cytoplasmic redox sensor WhiB3 with the DE gene lists indicates that disparate expression of virulence-related pathways regulated by these transcription factors between the two pathogens could have significant consequence for infection (47, 51, 52). Furthermore, PhoP, EspR and DosR are also significantly associated with the DE genes; these transcription factors are important for adaptation of *M. tuberculosis* to the intracellular environment and are functionally linked by such processes (Fig.1E) (53, 54).

The PhoPR two-component system has a major role in regulating the pathogenic phenotype of *M. tuberculosis* by controlling the expression of a variety of virulence-associated pathways including SL-1, DAT and PAT lipid production and the Type-VII secretion system ESX-1; mutations in the PhoPR system of *M. bovis* have been suggested to play a role in the host specificity between the bovine- and human-adapted mycobacterial species (23, 53, 55-57). Further investigation into the 72-gene regulon of PhoP identified 33 DE genes between the two species and these are presented in Fig.2A. The production of lipids SL-1 and PDIM is under PhoP regulation and is coupled within the *M. tuberculosis* cell; intriguingly *M. bovis* is reported to lack SL-1 in the cell envelope (58-60). In this study, the expression of genes associated with the biosynthesis of SL-1 (*e.g. papA1*, *papA2*, *pks2*, *mmpL8*) was at a higher level in *M. tuberculosis* and

444 conversely, genes associated with the biosynthesis of PDIM (*e.g. ppsA-E, lppX*) were
445 expressed at a higher level in *M. bovis* at the RNA and protein level (Fig.S5). SL-1 is one
446 of the most abundant lipids in the mycobacterial outer membrane, is unique to
447 pathogenic mycobacteria, is immunogenic, and is implicated in the alteration of phago-
448 lysosome fusion. Likewise, PDIM is required for mycobacterial virulence, facilitates
449 macrophage invasion and protects against reactive nitrogen species. The differential
450 expression of lipid-associated systems between the two species therefore presents
451 distinct lipid-repertoires to interact with the host that could affect the overall success of
452 infection (61-67).

453 The major antigens ESAT-6 and CFP10 are secreted by the ESX-1 secretion system
454 of *M. tuberculosis*, a system which has been implicated in mycobacterial escape from
455 the phagosome to the cytosol that results in a Type-I interferon response within the
456 infected macrophage (57, 68, 69). PhoP and EspR regulate the expression of ESX-1
457 secretion system-related genes and as stated are significantly associated with the DE
458 genes between the two pathogens; despite EspR being expressed to a higher level in *M.*
459 *tuberculosis* (Supp_III.xlsx), there is a significant upregulation of the ESX-1 secretion
460 system in *M. bovis* in comparison to *M. tuberculosis,* including ESX-1-related proteins
461 such as EsxA, EspA, EspC, EspD at both the transcriptional and translational level (55-57,
462 70, 71) (Fig.2B). Furthermore, PhoP was expressed to a higher level in *M. bovis*; this may
463 represent an attempt at a compensatory mechanism for aberrant PhoP signalling and
464 supports previous reports of suboptimal PhoP signalling in *M. bovis* (23, 59). Seven of 55
465 genes regulated by DosR were expressed higher at the RNA level in *M. tuberculosis*,

likely reflecting the intimate relationship of DosR and its associated regulon with that of PhoP/EspR/WhiB3 (Supp_IV.xlsx).

A "core" macrophage response common to infection with either species

117 strand-specific RNA-seq libraries were prepared from bovine alveolar infected macrophages that comprised *M. bovis*-, *M. tuberculosis*- and non-infected samples from each time point (0, 2, 6, 24 and 48 hpi) across 10 animals, with the exception of one animal that did not yield sufficient alveolar macrophages for *in vitro* infection at the 48 hour post-infection time point). Matched non-infected macrophage control samples were included for all infection time-points (Fig.S2). Quality control and mapping statistics can be found in Supp_V.csv and Fig.S5.

The comparison of *M. bovis*- or *M. tuberculosis*-infected macrophages with respect to non-infected macrophages revealed a sequential increase in the number of DE genes across the infection time-course, which peaked at 48 hpi and a larger number of DE genes were seen in *M. bovis*-infected macrophages with the exception of 6 hpi (Fig.3A, B, C, Supp_VI.csv); similar temporal expression profiles were previously reported in other *in vitro* bovine and human macrophage infection studies (42, 72-74). Comparison of these DE gene lists identified a subset of genes that displayed the same directionality and a similar magnitude of expression (Fig.4A) (Supp_VII.csv). The association of enriched pathways such as *Cytokine-cytokine receptor interaction, NOD-like receptor signalling* and *Jak-STAT signalling* with this gene subset suggests a robust

"core" macrophage response to infection with either mycobacterial species throughout the time course (Fig.4B). The core response includes numerous key genes known to be involved in the innate immune response against pathogenic mycobacteria such as: *CCL20* (75); *IL18,* which limits the growth of *M. tuberculosis* in human macrophages (76-78); anti-inflammatory *IL10* (79); and *NOS2*, polymorphisms of which are associated with susceptibility of Holstein cattle to bovine TB (80) (Fig.4C). Furthermore, the *HIF-1* signalling pathway was significantly enriched for the DE genes common to both infection series; this pathway is associated with regulating a switch in central glucose metabolism during high-energy demanding events, such as infection, in neutrophils and macrophages (81)(Fig.S6A).

DNA sensing and RIG-I like signalling pathways are found in the divergent response to infection with *M. tuberculosis* and *M. bovis*

Aside from the defined "core" response genes, there were larger numbers of DE genes in *M. bovis*-infected macrophages in contrast to *M. tuberculosis* infection, mainly at 24 hpi (1,313 versus 904 genes respectively) and 48 hpi (2,271 versus 1,037 genes respectively) (Fig.3A, B). Comparison of the relative change with respect to control between *M. bovis*- and *M. tuberculosis*-infected macrophages at each time-point revealed a statistically significant divergence in their responses at 48 hpi only associated with DE signatures from 703 genes (Fig.4A, Supp_VIII.csv). Analysis of the expression pattern of 576 of these genes with functional annotation across time revealed a greater magnitude of change in *M. bovis*- infected macrophages, where DE genes are up- or

509 down-regulated to a higher extent in *M. bovis*-infected macrophages or not significantly
510 changing at all in *M. tuberculosis*-infected macrophages (Fig.5C). Pathway enrichment
511 analysis revealed association of *ABC transporters* with the divergent annotated gene set
512 (Fig.5B); these are involved in cholesterol efflux from the cell, and manipulation of host
513 cell cholesterol transport and metabolism has been documented in *M. tuberculosis*
514 containing macrophages (82). A general dampening in the expression of cholesterol-
515 associated genes was noted in *M. bovis*-infected macrophages at 48 hpi (Fig.S6B).
516 Pathway enrichment analysis also associated *Cytosolic DNA-sensing* and *RIG-I-like*
517 *receptor signalling* with the 576 divergent genes (Fig.5C). Type-I interferons have been
518 associated with pathogenesis during *M. tuberculosis* infection and their production has
519 been found dependent on the mycobacterial ESX-1 secretion system and the cytosolic
520 sensing of extracellular *M. tuberculosis* DNA and subsequent cGAS-STING-dependent
521 signalling (83-86).

522 Overall, there is a stronger upregulation of genes encoding proteins involved in
523 *RIG-I-like* and *DNA-sensing* signalling in *M. bovis*-infected macrophages in comparison to
524 *M. tuberculosis*-infected macrophages at 48 hpi. These include genes encoding DNA
525 sensors such as MB21D1/cGAS, MDA5, IFI16, and DDX58/RIG-I, antiviral and MAVS-TBK1
526 interacting protein IFIT3, serine/threonine kinase TBK1, and key interferon-I
527 transcriptional regulators IRF3 and IRF7 that are all known to contribute to STING-
528 dependent induction of type-I interferons (Fig.5D, Fig.6) (87-89). Furthermore, genes
529 *LGP2, ISG15* and *TRIM25* that encode regulators of *DDX58*/*RIGI* gene expression are
530 upregulated in *M. bovis*-infected macrophages at 48 hpi (90). Likewise, downstream of

RIG-I, genes *IKBKB* and *IKB* are also expressed higher in *M. bovis*-infected macrophages along with *NFKB,* the gene encoding a key transcription factor that regulates the expression of inflammatory-related genes (89). Targets of NFKB such as *TNF, COX2, CXC40, MIP1a, IL8, IL12 and IL23a* are all expressed to a higher degree in *M. bovis*-infected macrophages with respect to *M. tuberculosis*-infected macrophages at 48 hpi (Fig.5D, Fig.6). A low level of reads mapped to the type I interferon genes *IFNAD* (orthologue of human *IFNA1*) and *IFNB1*, and only in a subset of animals at certain time points excluded these genes from DE analysis based on filtering criteria.

Independent of RIG-I signalling, genes involved in *DNA sensing* such as *TREX1*, which encodes a 3'-5' exonuclease that senses and degrades cytosolic DNA to prevent type I interferon production through the TBK1/STING/IRF3 pathway, and *OAS2* were also found expressed to a higher level in *M. bovis* containing macrophages (91). OAS2 is a double stranded RNA binding protein that generates 2'-5'- adenosine oligomers which activate RNase L resulting in the assembly of the NLRP3 inflammasome and IL-1b production (92, 93); genes *RNASEL*, *NLRP3* and non-canonical activation of the NLRP3 inflammasome *CASP4* were all found expressed to a higher level in *M. bovis*-infected macrophages 48hpi (94, 95) (Fig.4c, Fig.6). Taken together, these data highlight dissimilarity in the engagement between *M. bovis* and *M. tuberculosis* with the nucleic acid sensing system of the bovine macrophage, which in turn would influence downstream immune-related events, and ultimately infection outcome.

552 **Discussion**

553 The data we present here provides significant insight on the molecular basis of
554 host tropism between *M. tuberculosis* and *M. bovis* in the bovine host. Determining the
555 differences between the transcriptional and translational profiles of these two hallmark
556 mycobacterial strains highlighted variable expression of virulence-associated pathways
557 while a divergent transcriptional response to infection with either species in bovine
558 alveolar macrophages was observed 48 hpi. The ESX-1 secretion system of *M.*
559 *tuberculosis* is linked to its phagosomal escape during infection, a process that is
560 coupled to the triggering of DNA-sensing pathways in the cytosol of the host cell (83-
561 86). In this study, we found that the ESX-1 secretion system was expressed to a higher
562 level in *M. bovis* and a substantially stronger induction of DNA-sensing related pathways
563 was seen in bovine alveolar macrophages infected with *M. bovis* versus *M. tuberculosis*.
564 These data therefore suggest that *M. bovis* has a distinct engagement with the bovine
565 immune system and might thus be better able to drive phagosome rupture and
566 downstream immune signalling, leading to successful infection and ultimately disease.
567
568 In this study, we have taken advantage of both RNA-seq and SWATH mass
569 spectrometry to compare both the global transcriptional and translational expression
570 profiles of the human and bovine tubercle bacilli for definition of functional variation
571 between the two species that may explain their exhibited host preference. Other
572 studies have assessed in isolation either the transcriptome by microarray or the
573 proteome by shotgun mass spectrometry (27, 28, 96, 97); the resolution afforded by

574 both RNA-seq and SWATH mass spectrometry in comparison to previous studies has
575 allowed for the most complete dataset for *M. bovis* to date and the most complete
576 comparative dataset between the two pathogens. Although conducting a dual RNA-
577 sequencing study may facilitate simultaneous assessment of the transcriptional
578 response of both the host macrophage and invading mycobacteria during infection, this
579 technique is limited with regards to the proportion of the bacterial-to-host
580 transcriptome ratio in the resulting data and it does not allow for the accurate capture
581 of both the global transcriptomic and proteomic dynamics of the mycobacteria during
582 infection (98). As we aimed to investigate the early response of the macrophage to
583 infection with both mycobacterial species, we believe the overall expression profiles
584 measured in this study *in vitro* more realistically represent the bacterial phenotypes first
585 encountered by the host cell. Lastly, we focused on *M. tuberculosis* H37Rv and *M. bovis*
586 AF2122/97 as they are widely used reference strains and they have been previously
587 used to demonstrate the attenuation of *M. tuberculosis* in the bovine host (1, 9).
588
589 The relatively small number of DE genes at both the RNA and protein level
590 between *M. bovis* and *M. tuberculosis* highlights the close genetic relationship between
591 the two pathogens. That being said, assessment of these DE genes supports our
592 hypothesis that subtle genetic changes between the two species result in divergent
593 phenotypes driven by differential expression of major virulence associated factors and
594 pathways. We found that transcription factors PhoP, WhiB3 and DosR are significantly
595 associated with the DE genes between the two species and these are functionally linked

596 by processes that govern the adaptation of *M. tuberculosis* to the intracellular
597 environment (53, 54). The PhoPR two-component system is important for *M.*
598 *tuberculosis* infection and it has been suggested that mutations in PhoR attenuate
599 animal-adapted *M. bovis* in humans (23, 99-105). PhoP regulates the production of
600 virulence associated cell wall lipids and controls the expression of EspA, an ESX-1
601 secretion pathway related protein involved in the secretion of the major antigen
602 EsxA/ESAT6 (55, 56, 70, 71). We found that the ESX-1 secretion system is expressed to a
603 higher degree at both the RNA and protein level in *M. bovis* in comparison to *M.*
604 *tuberculosis*; differences in ESX-1 secretion system expression between the two
605 pathogens may be a consequence of a SNP in the promoter of the *whiB6* gene in *M.*
606 *tuberculosis* H37Rv or attributed to attenuated PhoPR signalling in *M. bovis* (56). There
607 is an emerging body of evidence showing that *M. tuberculosis* can rupture the
608 phagosome membrane through the action of the ESX-1 secretion system and that the
609 activation of cytosolic DNA-sensing pathways and the production of Type-I interferons is
610 dependent on ESX-1 expression (83-86). Based on our data, we speculate that alternate
611 transcriptional regulation between *M. tuberculosis* and *M. bovis* as a consequence of
612 genetic variation may represent differential priming events in preparation for the initial
613 interactions of both species with their respective host immune systems. For example,
614 increased expression ESX-1 secretion system may facilitate faster escape of *M. bovis*
615 from the phagosome into the cytosol in contrast to *M. tuberculosis*, triggering DNA-
616 sensing pathways and increased type I interferon production (68, 85, 106).
617

618 To determine the impact of pathogen variation on host response, we conducted
619 an experimental infection of primary bovine alveolar macrophages with *M. tuberculosis*
620 and *M. bovis* and tracked the transcriptional response to infection. The bovine alveolar
621 macrophage response to infection with either pathogen was strikingly similar over the
622 first 24 hours of infection. Notably, a "core" macrophage response displayed
623 enrichment for differentially expressed genes involved in pathogen recognition, innate
624 cell signalling, and cytokine and chemokine production illustrating the initiation of host
625 innate defence mechanisms in response to infection with *M. bovis* and *M. tuberculosis*.
626 One of the most striking observations is that divergence in macrophage gene expression
627 profiles between *M. bovis* and *M. tuberculosis* infections only occurs after 24 h, with *M.*
628 *bovis* infection eliciting a stronger response in comparison to *M. tuberculosis*. At 48 hpi,
629 enrichment for *DNA sensing* was found for 576 annotated genes that show divergent
630 expression patterns between the two infection models. The innate immune system
631 detects exogenous nucleic acid within the cell through pattern recognition receptors
632 (PRRs) that include Absent in Melanoma 2 (AIM2)-like receptors (ALRs) with Pyrin and
633 HIN domains (PYHIN proteins), *e.g.* IFI16 (107-109). Other DNA-sensing proteins include
634 cytosolic RIG-I-like receptors (RLR), (*e.g.* RIG-I, MDA5, LGP2), exonucleases, synthetases,
635 and cyclic GMP-AMP synthases (*e.g.* TREX1, OAS2 and cGAS) (83, 91, 93, 110, 111). A
636 stronger transcriptional induction of genes associated with cGAS-STING dependent
637 signalling was seen in macrophages infected with *M. bovis* including *MB21D1/cGAS* and
638 downstream effectors *TBK1* and *IRF3* (Fig.6). cGAS has a central role during *M.*
639 *tuberculosis* infection*;* 48-72 hpi cGAS senses *M. tuberculosis* in the host cell cytosol and

in turn signals through STING to drive type-I interferon production (Fig.6) (68, 83-86, 112). Surprisingly, the cGAS-STING axis was not the only PRR pathway found upregulated during mycobacterial infection as *RIG-I like signalling* pathway was also observed to be enriched at 48 hpi, with genes encoding TREX1, OAS2, and RLR receptors RIG-I, MDA5 and LGP2 also found expressed to a higher level in *M.* bovis-infected macrophages. As we hypothesised that the variation in host response at 48 hpi, and ultimately host tropism, is driven by differential expression of virulence factors between *M. bovis* and *M. tuberculosis,* the identification of an increase in expression of DNA-sensing related pathways in *M. bovis*-infected macrophages at 48 hpi coincides with the differential expression of the ESX-1 secretion system between the two pathogens. A further role for the ESX-1 secretion system in host-pathogen interactions is described through the activation of the host NLRP3 inflammasome and the production of IL-1b (113-116). Transcriptional signals associated with the NLRP3 inflammasome were higher in *M. bovis*-infected macrophages at 48 hpi along with the increased expression of *CASP4*, an NLRP3 inflammasome activator, which has a central role in mediating the response to *Legionella*, *Yersinia* and *Salmonella* bacterial infection in primary human macrophages and that has been found upregulated in the necrotic granuloma model of mice and lymph nodes of TB patients (92, 117-119). Altogether, these data therefore suggest that not only does mycobacterial infection in the bovine macrophage trigger an increase in the transcription of the cGAS/STING/IRF3 pathway previously characterised as responsible for type-I interferon production during *M. tuberculosis* infection, it also triggers alteration in the transcription of genes encoding auxiliary DNA sensing RLR

662 receptors including RIG-I, MDA5 and TREX1, that likewise converge to signal through the
663 STING complex (Fig.6). Furthermore, the data highlights that *M. bovis* drives a stronger
664 transcriptional response in the aforementioned pathways in the bovine alveolar
665 macrophage at 48 hpi in comparison to *M. tuberculosis,* again highlighting a distinct
666 relationship between the bovine pathogen and the bovine host.
667
668 Altogether, the upregulation of the ESX1 secretion system at both the RNA and
669 protein level in *M. bovis* with the observed upregulation of DNA-sensing pathways and
670 the NLRP3/IL-1b pathway in *M. bovis*-infected macrophages suggests that the
671 expression level of virulence factors, rather than the presence or absence of them
672 between the highly related *M. bovis* and *M. tuberculosis*, drives divergent host
673 responses and influences infection outcome overall. Indeed, the idea of a 'perfect
674 balance' with regards to the expression of mycobacterial virulence factors is reflected in
675 the findings that production of IFN-β1 in monocyte-derived macrophages is strain
676 dependent amongst the *M. tuberculosis* lineages (120). That being said, we cannot
677 disregard that genetic differences between the bovine and human host may play a
678 factor. As the innate immune response in different mammals can vary, diversity in the
679 expression and structure in key innate immune genes and engagement with pathogen
680 factors must play major roles in host specificity and the outcome of pathogen encounter
681 (121). In this regard, it is interesting to note that the bovine PYHIN locus contains only
682 *IFI16* (bovine PYHIN) and cattle are the only mammals to date found to encode a single
683 member of PYHIN protein family; in contrast, humans have four genes, and mice 13

684 genes (122). Furthermore, polymorphisms in *NLRP3* have been found to influence host
685 susceptibility to *M. tuberculosis* infection, its induction is associated with the
686 mycobacterial ESX-1 secretion system, and bovine and human NLRP3 proteins share
687 83% sequence identity (123). Further comparative studies of human and bovine genetics
688 will ultimately aid in unravelling the complex differential host response to infection with
689 both pathogens. Moreover, we cannot overlook other virulence-associated factors
690 besides the ESX-1 secretion system that differ in expression or sequence between
691 *M. bovis* and *M. tuberculosis.* Indeed, antigens MBP83 and MBP70, that show
692 constitutive upregulation in *M. bovis* versus *M. tuberculosis* and pathways such as ESX-3
693 and Mce-1 were also found differentially expressed between the two pathogens at both
694 the transcriptional and translational level during *in vitro* growth in this study
695 (Supp_III.xlsx) (47, 124).
696
697 In conclusion, we found that *M. tuberculosis* H37Rv and *M. bovis* AF2122/97
698 induce divergent responses in infected bovine alveolar macrophages, a consequence of
699 the differential expression of key mycobacterial virulence-associated pathways. Our
700 work demonstrates the specificity of mycobacterial host-pathogen interaction and
701 indicates how the subtle interplay between the phenotype of the invading mycobacteria
702 and the subsequent host response may underpin host specificity amongst members of
703 the MTBC.
704
705

706 **Acknowledgements:**

707 We would like to thank Dr. Christina Ludwig for help with the SWATH mass

708 spectrometry measurements and Dr. Maximiliano Gutierrez for valuable input and

709 discussion. We gratefully acknowledge funding from Science Foundation Ireland through

710 SFI Investigator Awards 08/IN.1/B2038 and 15/IA/3154; the European Commission's

711 H2020 program grant number 643381 (TBVAC2020); Wellcome Trust PhD awards

712 097429/Z/11/Z (K.R-A.) and 102395/Z/13/Z (A.S.). The work was further supported by

713 funding from SystemsX.ch/TbX (R.A.) and a research grant from Institut Mérieux (R.A.).

714

References

1. Whelan AO, Coad M, Cockle PJ, Hewinson G, Vordermeier M, Gordon SV. 2010. Revisiting host preference in the Mycobacterium tuberculosis complex: experimental infection shows M. tuberculosis H37Rv to be avirulent in cattle. PLoS One 5:e8527.

2. Garnier T, Eiglmeier K, Camus JC, Medina N, Mansoor H, Pryor M, Duthoy S, Grondin S, Lacroix C, Monsempe C, Simon S, Harris B, Atkin R, Doggett J, Mayes R, Keating L, Wheeler PR, Parkhill J, Barrell BG, Cole ST, Gordon SV, Hewinson RG. 2003. The complete genome sequence of Mycobacterium bovis. Proc Natl Acad Sci U S A 100:7877-82.

3. Coscolla M, Gagneux S. 2014. Consequences of genomic diversity in Mycobacterium tuberculosis. Semin Immunol 26:431-44.

4. Malone KM, Gordon SV. 2017. Mycobacterium tuberculosis Complex Members Adapted to Wild and Domestic Animals. Adv Exp Med Biol 1019:135-154.

5. WHO. 2017. Global tuberculosis report. http://www.who.int/tb/publications/global_report/en/. Accessed

6. Abernethy DA, Upton P, Higgins IM, McGrath G, Goodchild AV, Rolfe SJ, Broughan JM, Downs SH, Clifton-Hadley R, Menzies FD, de la Rua-Domenech R, Blissitt MJ, Duignan A, More SJ. 2013. Bovine tuberculosis trends in the UK and the Republic of Ireland, 1995-2010. Vet Rec 172:312.

7. Mableson HE, Okello A, Picozzi K, Welburn SC. 2014. Neglected zoonotic diseases-the long and winding road to advocacy. PLoS Negl Trop Dis 8:e2800.

737 8. Heath D. 2013. Response to FOI request about various bovine TB costs from
738 2008 to 2013. In: Department for Environment, F A R A.
739 9. Bernardo Villarreal-Ramos SB, Adam Whelan, Sebastien Holbert, Florence
740 Carreras, Francisco J. Salguero, Bhagwati Khatri, Kerri M. Malone, Kevin Rue-
741 Albrecht, Ronan Shaughnessy, Alicia M. Smyth, Gobena Ameni, Abraham Aseffa,
742 Pierre Sarradin, Nathalie Winter, Martin Vordermeier, Stephen V. Gordon. 2017.
743 Experimental infection of cattle with Mycobacterium tuberculosis isolates shows
744 the attenuation of the human tubercle bacillus for cattle. bioRxiv
745 doi:https://doi.org/10.1101/202663.
746 10. Francis J. 1950. Control of infection with the bovine tubercle bacillus. Lancet
747 1:34-9.
748 11. Magnus K. 1966. Epidemiological Basis of Tuberculosis Eradication 3. Risk of
749 Pulmonary Tuberculosis after Human and Bovine Infection. Bull World Health
750 Organ 35:483-508.
751 12. McNab F, Mayer-Barber K, Sher A, Wack A, O'Garra A. 2015. Type I interferons in
752 infectious disease. Nat Rev Immunol 15:87-103.
753 13. Welin A, Lerm M. 2012. Inside or outside the phagosome? The controversy of
754 the intracellular localization of Mycobacterium tuberculosis. Tuberculosis (Edinb)
755 92:113-20.
756 14. Dorhoi A, Kaufmann SH. 2014. Perspectives on host adaptation in response to
757 Mycobacterium tuberculosis: modulation of inflammation. Semin Immunol
758 26:533-42.

759 15. Magee DA, Conlon KM, Nalpas NC, Browne JA, Pirson C, Healy C, McLoughlin KE,
760 Chen J, Vordermeier HM, Gormley E, MacHugh DE, Gordon SV. 2014. Innate
761 cytokine profiling of bovine alveolar macrophages reveals commonalities and
762 divergence in the response to Mycobacterium bovis and Mycobacterium
763 tuberculosis infection. Tuberculosis (Edinb) 94:441-50.
764 16. Piercy J, Werling D, Coffey TJ. 2007. Differential responses of bovine
765 macrophages to infection with bovine-specific and non-bovine specific
766 mycobacteria. Tuberculosis (Edinb) 87:415-20.
767 17. Marino S, Cilfone NA, Mattila JT, Linderman JJ, Flynn JL, Kirschner DE. 2015.
768 Macrophage polarization drives granuloma outcome during Mycobacterium
769 tuberculosis infection. Infect Immun 83:324-38.
770 18. Rajaram MV, Ni B, Dodd CE, Schlesinger LS. 2014. Macrophage
771 immunoregulatory pathways in tuberculosis. Semin Immunol 26:471-85.
772 19. Cassidy JP, Martineau AR. 2014. Innate resistance to tuberculosis in man, cattle
773 and laboratory animal models: nipping disease in the bud? J Comp Pathol
774 151:291-308.
775 20. Widdison S, Watson M, Piercy J, Howard C, Coffey TJ. 2008. Granulocyte
776 chemotactic properties of M. tuberculosis versus M. bovis-infected bovine
777 alveolar macrophages. Mol Immunol 45:740-9.
778 21. Malone KM, Farrell D, Stuber TP, Schubert OT, Aebersold R, Robbe-Austerman S,
779 Gordon SV. 2017. Updated Reference Genome Sequence and Annotation of
780 Mycobacterium bovis AF2122/97. Genome Announc 5.

781 22. Cole ST, Brosch R, Parkhill J, Garnier T, Churcher C, Harris D, Gordon SV,
782 Eiglmeier K, Gas S, Barry CE, 3rd, Tekaia F, Badcock K, Basham D, Brown D,
783 Chillingworth T, Connor R, Davies R, Devlin K, Feltwell T, Gentles S, Hamlin N,
784 Holroyd S, Hornsby T, Jagels K, Krogh A, McLean J, Moule S, Murphy L, Oliver K,
785 Osborne J, Quail MA, Rajandream MA, Rogers J, Rutter S, Seeger K, Skelton J,
786 Squares R, Squares S, Sulston JE, Taylor K, Whitehead S, Barrell BG. 1998.
787 Deciphering the biology of Mycobacterium tuberculosis from the complete
788 genome sequence. Nature 393:537-44.
789 23. Gonzalo-Asensio J, Malaga W, Pawlik A, Astarie-Dequeker C, Passemar C,
790 Moreau F, Laval F, Daffe M, Martin C, Brosch R, Guilhot C. 2014. Evolutionary
791 history of tuberculosis shaped by conserved mutations in the PhoPR virulence
792 regulator. Proc Natl Acad Sci U S A 111:11491-6.
793 24. Malaga W, Constant P, Euphrasie D, Cataldi A, Daffe M, Reyrat JM, Guilhot C.
794 2008. Deciphering the genetic bases of the structural diversity of phenolic
795 glycolipids in strains of the Mycobacterium tuberculosis complex. J Biol Chem
796 283:15177-84.
797 25. Sohaskey CD, Modesti L. 2009. Differences in nitrate reduction between
798 Mycobacterium tuberculosis and Mycobacterium bovis are due to differential
799 expression of both narGHJI and narK2. FEMS Microbiol Lett 290:129-34.
800 26. Stermann M, Bohrssen A, Diephaus C, Maass S, Bange FC. 2003. Polymorphic
801 nucleotide within the promoter of nitrate reductase (NarGHJI) is specific for
802 Mycobacterium tuberculosis. J Clin Microbiol 41:3252-9.

27. Golby P, Hatch KA, Bacon J, Cooney R, Riley P, Allnutt J, Hinds J, Nunez J, Marsh PD, Hewinson RG, Gordon SV. 2007. Comparative transcriptomics reveals key gene expression differences between the human and bovine pathogens of the Mycobacterium tuberculosis complex. Microbiology 153:3323-36.

28. Rehren G, Walters S, Fontan P, Smith I, Zarraga AM. 2007. Differential gene expression between Mycobacterium bovis and Mycobacterium tuberculosis. Tuberculosis (Edinb) 87:347-59.

29. Gillet LC, Navarro P, Tate S, Rost H, Selevsek N, Reiter L, Bonner R, Aebersold R. 2012. Targeted data extraction of the MS/MS spectra generated by data-independent acquisition: a new concept for consistent and accurate proteome analysis. Mol Cell Proteomics 11:O111 016717.

30. Andrews S. 2010. A quality control tool for high throughput sequence data.

31. Lunter G, Goodson M. 2011. Stampy: a statistical algorithm for sensitive and fast mapping of Illumina sequence reads. Genome Res 21:936-9.

32. Liao Y, Smyth GK, Shi W. 2014. featureCounts: an efficient general purpose program for assigning sequence reads to genomic features. Bioinformatics 30:923-30.

33. Love MI, Huber W, Anders S. 2014. Moderated estimation of fold change and dispersion for RNA-seq data with DESeq2. Genome Biol 15:550.

34. Wagner GP, Kin K, Lynch VJ. 2012. Measurement of mRNA abundance using RNA-seq data: RPKM measure is inconsistent among samples. Theory Biosci 131:281-5.

825 35. Minch KJ, Rustad TR, Peterson EJ, Winkler J, Reiss DJ, Ma S, Hickey M, Brabant W,
826 Morrison B, Turkarslan S, Mawhinney C, Galagan JE, Price ND, Baliga NS,
827 Sherman DR. 2015. The DNA-binding network of Mycobacterium tuberculosis.
828 Nat Commun 6:5829.
829 36. Rustad TR, Minch KJ, Ma S, Winkler JK, Hobbs S, Hickey M, Brabant W, Turkarslan
830 S, Price ND, Baliga NS, Sherman DR. 2014. Mapping and manipulating the
831 Mycobacterium tuberculosis transcriptome using a transcription factor
832 overexpression-derived regulatory network. Genome Biol 15:502.
833 37. Turkarslan S, Peterson EJ, Rustad TR, Minch KJ, Reiss DJ, Morrison R, Ma S, Price
834 ND, Sherman DR, Baliga NS. 2015. A comprehensive map of genome-wide gene
835 regulation in Mycobacterium tuberculosis. Sci Data 2:150010.
836 38. Rost HL, Rosenberger G, Navarro P, Gillet L, Miladinovic SM, Schubert OT, Wolski
837 W, Collins BC, Malmstrom J, Malmstrom L, Aebersold R. 2014. OpenSWATH
838 enables automated, targeted analysis of data-independent acquisition MS data.
839 Nat Biotechnol 32:219-23.
840 39. Schubert OT, Ludwig C, Kogadeeva M, Zimmermann M, Rosenberger G,
841 Gengenbacher M, Gillet LC, Collins BC, Rost HL, Kaufmann SH, Sauer U,
842 Aebersold R. 2015. Absolute Proteome Composition and Dynamics during
843 Dormancy and Resuscitation of Mycobacterium tuberculosis. Cell Host Microbe
844 18:96-108.
845 40. Schubert OT, Mouritsen J, Ludwig C, Rost HL, Rosenberger G, Arthur PK, Claassen
846 M, Campbell DS, Sun Z, Farrah T, Gengenbacher M, Maiolica A, Kaufmann SH,

Moritz RL, Aebersold R. 2013. The Mtb proteome library: a resource of assays to quantify the complete proteome of Mycobacterium tuberculosis. Cell Host Microbe 13:602-12.

41. Choi M, Chang CY, Clough T, Broudy D, Killeen T, MacLean B, Vitek O. 2014. MSstats: an R package for statistical analysis of quantitative mass spectrometry-based proteomic experiments. Bioinformatics 30:2524-6.

42. Nalpas NC, Magee DA, Conlon KM, Browne JA, Healy C, McLoughlin KE, Rue-Albrecht K, McGettigan PA, Killick KE, Gormley E, Gordon SV, MacHugh DE. 2015. RNA sequencing provides exquisite insight into the manipulation of the alveolar macrophage by tubercle bacilli. Sci Rep 5:13629.

43. Dobin A, Davis CA, Schlesinger F, Drenkow J, Zaleski C, Jha S, Batut P, Chaisson M, Gingeras TR. 2013. STAR: ultrafast universal RNA-seq aligner. Bioinformatics 29:15-21.

44. Robinson MD, McCarthy DJ, Smyth GK. 2010. edgeR: a Bioconductor package for differential expression analysis of digital gene expression data. Bioinformatics 26:139-40.

45. Hochberg YBaY. 1995. Controlling the False Discovery Rate: A Practical and Powerful Approach to Multiple Testing. Journal of the Royal Statistical Society 57:289-300.

46. Foroushani AB, Brinkman FS, Lynn DJ. 2013. Pathway-GPS and SIGORA: identifying relevant pathways based on the over-representation of their gene-pair signatures. PeerJ 1:e229.

869 47. Veyrier F, Said-Salim B, Behr MA. 2008. Evolution of the mycobacterial SigK
870 regulon. J Bacteriol 190:1891-9.
871 48. Maier T, Guell M, Serrano L. 2009. Correlation of mRNA and protein in complex
872 biological samples. FEBS Lett 583:3966-73.
873 49. Vogel C, Abreu Rde S, Ko D, Le SY, Shapiro BA, Burns SC, Sandhu D, Boutz DR,
874 Marcotte EM, Penalva LO. 2010. Sequence signatures and mRNA concentration
875 can explain two-thirds of protein abundance variation in a human cell line. Mol
876 Syst Biol 6:400.
877 50. Cortes T, Schubert OT, Banaei-Esfahani A, Collins BC, Aebersold R, Young DB.
878 2017. Delayed effects of transcriptional responses in Mycobacterium
879 tuberculosis exposed to nitric oxide suggest other mechanisms involved in
880 survival. Sci Rep 7:8208.
881 51. Mehta M, Rajmani RS, Singh A. 2015. Mycobacterium tuberculosis WhiB3
882 responds to vacuolar pH- induced changes in mycothiol redox potential to
883 modulate phagosomal maturation and virulence. J Biol Chem
884 doi:10.1074/jbc.M115.684597.
885 52. Gebhard S, Humpel A, McLellan AD, Cook GM. 2008. The alternative sigma factor
886 SigF of Mycobacterium smegmatis is required for survival of heat shock, acidic
887 pH and oxidative stress. Microbiology 154:2786-95.
888 53. Singh A, Crossman DK, Mai D, Guidry L, Voskuil MI, Renfrow MB, Steyn AJ. 2009.
889 Mycobacterium tuberculosis WhiB3 maintains redox homeostasis by regulating

890 virulence lipid anabolism to modulate macrophage response. PLoS Pathog
891 5:e1000545.
892 54. Sherman DR, Voskuil M, Schnappinger D, Liao R, Harrell MI, Schoolnik GK. 2001.
893 Regulation of the Mycobacterium tuberculosis hypoxic response gene encoding
894 alpha -crystallin. Proc Natl Acad Sci U S A 98:7534-9.
895 55. Chen JM, Zhang M, Rybniker J, Basterra L, Dhar N, Tischler AD, Pojer F, Cole ST.
896 2013. Phenotypic profiling of Mycobacterium tuberculosis EspA point mutants
897 reveals that blockage of ESAT-6 and CFP-10 secretion in vitro does not always
898 correlate with attenuation of virulence. J Bacteriol 195:5421-30.
899 56. Solans L, Aguilo N, Samper S, Pawlik A, Frigui W, Martin C, Brosch R, Gonzalo-
900 Asensio J. 2014. A specific polymorphism in Mycobacterium tuberculosis H37Rv
901 causes differential ESAT-6 expression and identifies WhiB6 as a novel ESX-1
902 component. Infect Immun 82:3446-56.
903 57. Simeone R, Bottai D, Brosch R. 2009. ESX/type VII secretion systems and their
904 role in host-pathogen interaction. Curr Opin Microbiol 12:4-10.
905 58. Goren MB. 1970. Sulfolipid I of Mycobacterium tuberculosis, strain H37Rv. I.
906 Purification and properties. Biochim Biophys Acta 210:116-26.
907 59. Gonzalo Asensio J, Maia C, Ferrer NL, Barilone N, Laval F, Soto CY, Winter N,
908 Daffe M, Gicquel B, Martin C, Jackson M. 2006. The virulence-associated two-
909 component PhoP-PhoR system controls the biosynthesis of polyketide-derived
910 lipids in Mycobacterium tuberculosis. J Biol Chem 281:1313-6.

911 60. Jain M, Petzold CJ, Schelle MW, Leavell MD, Mougous JD, Bertozzi CR, Leary JA,
912 Cox JS. 2007. Lipidomics reveals control of Mycobacterium tuberculosis virulence
913 lipids via metabolic coupling. Proc Natl Acad Sci U S A 104:5133-8.
914 61. Seeliger JC, Holsclaw CM, Schelle MW, Botyanszki Z, Gilmore SA, Tully SE,
915 Niederweis M, Cravatt BF, Leary JA, Bertozzi CR. 2012. Elucidation and chemical
916 modulation of sulfolipid-1 biosynthesis in Mycobacterium tuberculosis. J Biol
917 Chem 287:7990-8000.
918 62. Yu J, Tran V, Li M, Huang X, Niu C, Wang D, Zhu J, Wang J, Gao Q, Liu J. 2012.
919 Both phthiocerol dimycocerosates and phenolic glycolipids are required for
920 virulence of Mycobacterium marinum. Infect Immun 80:1381-9.
921 63. Day TA, Mittler JE, Nixon MR, Thompson C, Miner MD, Hickey MJ, Liao RP, Pang
922 JM, Shayakhmetov DM, Sherman DR. 2014. Mycobacterium tuberculosis strains
923 lacking surface lipid phthiocerol dimycocerosate are susceptible to killing by an
924 early innate host response. Infect Immun 82:5214-22.
925 64. Zhang L, English D, Andersen BR. 1991. Activation of human neutrophils by
926 Mycobacterium tuberculosis-derived sulfolipid-1. J Immunol 146:2730-6.
927 65. Brodin P, Poquet Y, Levillain F, Peguillet I, Larrouy-Maumus G, Gilleron M, Ewann
928 F, Christophe T, Fenistein D, Jang J, Jang MS, Park SJ, Rauzier J, Carralot JP,
929 Shrimpton R, Genovesio A, Gonzalo-Asensio JA, Puzo G, Martin C, Brosch R,
930 Stewart GR, Gicquel B, Neyrolles O. 2010. High content phenotypic cell-based
931 visual screen identifies Mycobacterium tuberculosis acyltrehalose-containing
932 glycolipids involved in phagosome remodeling. PLoS Pathog 6:e1001100.

933 66. Rousseau C, Winter N, Pivert E, Bordat Y, Neyrolles O, Ave P, Huerre M, Gicquel
934 B, Jackson M. 2004. Production of phthiocerol dimycocerosates protects
935 Mycobacterium tuberculosis from the cidal activity of reactive nitrogen
936 intermediates produced by macrophages and modulates the early immune
937 response to infection. Cell Microbiol 6:277-87.
938 67. Astarie-Dequeker C, Le Guyader L, Malaga W, Seaphanh FK, Chalut C, Lopez A,
939 Guilhot C. 2009. Phthiocerol dimycocerosates of M. tuberculosis participate in
940 macrophage invasion by inducing changes in the organization of plasma
941 membrane lipids. PLoS Pathog 5:e1000289.
942 68. Simeone R, Bobard A, Lippmann J, Bitter W, Majlessi L, Brosch R, Enninga J. 2012.
943 Phagosomal rupture by Mycobacterium tuberculosis results in toxicity and host
944 cell death. PLoS Pathog 8:e1002507.
945 69. Simeone R, Bottai D, Frigui W, Majlessi L, Brosch R. 2015. ESX/type VII secretion
946 systems of mycobacteria: Insights into evolution, pathogenicity and protection.
947 Tuberculosis (Edinb) 95 Suppl 1:S150-4.
948 70. Chim N, Johnson PM, Goulding CW. 2014. Insights into redox sensing
949 metalloproteins in Mycobacterium tuberculosis. J Inorg Biochem 133:118-26.
950 71. Cao G, Howard ST, Zhang P, Wang X, Chen XL, Samten B, Pang X. 2015. EspR, a
951 regulator of the ESX-1 secretion system in Mycobacterium tuberculosis, is
952 directly regulated by the two-component systems MprAB and PhoPR.
953 Microbiology 161:477-89.

954 72. Bullard JH, Purdom E, Hansen KD, Dudoit S. 2010. Evaluation of statistical
955 methods for normalization and differential expression in mRNA-Seq
956 experiments. BMC Bioinformatics 11:94.
957 73. Tarazona S, Garcia-Alcalde F, Dopazo J, Ferrer A, Conesa A. 2011. Differential
958 expression in RNA-seq: a matter of depth. Genome Res 21:2213-23.
959 74. Rue-Albrecht K, Magee DA, Killick KE, Nalpas NC, Gordon SV, MacHugh DE. 2014.
960 Comparative functional genomics and the bovine macrophage response to
961 strains of the mycobacterium genus. Front Immunol 5:536.
962 75. Rivero-Lezcano OM, Gonzalez-Cortes C, Reyes-Ruvalcaba D, Diez-Tascon C. 2010.
963 CCL20 is overexpressed in Mycobacterium tuberculosis-infected monocytes and
964 inhibits the production of reactive oxygen species (ROS). Clin Exp Immunol
965 162:289-97.
966 76. Robinson CM, Jung JY, Nau GJ. 2012. Interferon-gamma, tumor necrosis factor,
967 and interleukin-18 cooperate to control growth of Mycobacterium tuberculosis
968 in human macrophages. Cytokine 60:233-41.
969 77. Lee SH, Choi IH, Jeon YK, Park SJ, Lee HK, Lee YM, Chang CL, Kim YS, Lee MK, Park
970 SK. 2011. Association between the interleukin-18 promoter polymorphism and
971 pulmonary tuberculosis in a Korean population. Int J Tuberc Lung Dis 15:1246-51,
972 i.
973 78. Han M, Yue J, Lian YY, Zhao YL, Wang HX, Liu LR. 2011. Relationship between
974 single nucleotide polymorphism of interleukin-18 and susceptibility to

pulmonary tuberculosis in the Chinese Han population. Microbiol Immunol 55:388-93.

79. Redford PS, Murray PJ, O'Garra A. 2011. The role of IL-10 in immune regulation during M. tuberculosis infection. Mucosal Immunol 4:261-70.

80. Cheng Y, Huang C, Tsai HJ. 2016. Relationship of bovine NOS2 gene polymorphisms to the risk of bovine tuberculosis in Holstein cattle. J Vet Med Sci 78:281-6.

81. Kelly B, O'Neill LA. 2015. Metabolic reprogramming in macrophages and dendritic cells in innate immunity. Cell Res 25:771-84.

82. Lovewell RR, Sassetti CM, VanderVen BC. 2016. Chewing the fat: lipid metabolism and homeostasis during M. tuberculosis infection. Curr Opin Microbiol 29:30-6.

83. Collins AC, Cai H, Li T, Franco LH, Li XD, Nair VR, Scharn CR, Stamm CE, Levine B, Chen ZJ, Shiloh MU. 2015. Cyclic GMP-AMP Synthase Is an Innate Immune DNA Sensor for Mycobacterium tuberculosis. Cell Host Microbe 17:820-8.

84. Dey B, Dey RJ, Cheung LS, Pokkali S, Guo H, Lee JH, Bishai WR. 2015. A bacterial cyclic dinucleotide activates the cytosolic surveillance pathway and mediates innate resistance to tuberculosis. Nat Med 21:401-6.

85. Wassermann R, Gulen MF, Sala C, Perin SG, Lou Y, Rybniker J, Schmid-Burgk JL, Schmidt T, Hornung V, Cole ST, Ablasser A. 2015. Mycobacterium tuberculosis Differentially Activates cGAS- and Inflammasome-Dependent Intracellular Immune Responses through ESX-1. Cell Host Microbe 17:799-810.

997 86. Watson RO, Bell SL, MacDuff DA, Kimmey JM, Diner EJ, Olivas J, Vance RE,
998 Stallings CL, Virgin HW, Cox JS. 2015. The Cytosolic Sensor cGAS Detects
999 Mycobacterium tuberculosis DNA to Induce Type I Interferons and Activate
1000 Autophagy. Cell Host Microbe 17:811-9.
1001 87. Kato H, Oh SW, Fujita T. 2017. RIG-I-Like Receptors and Type I
1002 Interferonopathies. J Interferon Cytokine Res 37:207-213.
1003 88. Keating SE, Baran M, Bowie AG. 2011. Cytosolic DNA sensors regulating type I
1004 interferon induction. Trends Immunol 32:574-81.
1005 89. Zevini A, Olagnier D, Hiscott J. 2017. Crosstalk between Cytoplasmic RIG-I and
1006 STING Sensing Pathways. Trends Immunol 38:194-205.
1007 90. Komuro A, Bamming D, Horvath CM. 2008. Negative regulation of cytoplasmic
1008 RNA-mediated antiviral signaling. Cytokine 43:350-8.
1009 91. Yan N, Regalado-Magdos AD, Stiggelbout B, Lee-Kirsch MA, Lieberman J. 2010.
1010 The cytosolic exonuclease TREX1 inhibits the innate immune response to human
1011 immunodeficiency virus type 1. Nat Immunol 11:1005-13.
1012 92. Chakrabarti A, Banerjee S, Franchi L, Loo YM, Gale M, Jr., Nunez G, Silverman RH.
1013 2015. RNase L activates the NLRP3 inflammasome during viral infections. Cell
1014 Host Microbe 17:466-77.
1015 93. Ting JP, Duncan JA, Lei Y. 2010. How the noninflammasome NLRs function in the
1016 innate immune system. Science 327:286-90.

1017 94. Vigano E, Diamond CE, Spreafico R, Balachander A, Sobota RM, Mortellaro A.
1018 2015. Human caspase-4 and caspase-5 regulate the one-step non-canonical
1019 inflammasome activation in monocytes. Nat Commun 6:8761.
1020 95. Schmid-Burgk JL, Gaidt MM, Schmidt T, Ebert TS, Bartok E, Hornung V. 2015.
1021 Caspase-4 mediates non-canonical activation of the NLRP3 inflammasome in
1022 human myeloid cells. Eur J Immunol 45:2911-7.
1023 96. Beltran PK, Gutierrez-Ortega A, Puebla-Perez AM, Gutierrez-Pabello JA, Flores-
1024 Valdez MA, Hernandez-Gutierrez R, Martinez-Velazquez M, Alvarez AH. 2011.
1025 Identification of immunodominant antigens of Mycobacterium bovis by
1026 expression library immunization. Vet J 190:181-3.
1027 97. Zheng J, Liu L, Wei C, Leng W, Yang J, Li W, Wang J, Jin Q. 2012. A comprehensive
1028 proteomic analysis of Mycobacterium bovis bacillus Calmette-Guerin using high
1029 resolution Fourier transform mass spectrometry. J Proteomics 77:357-71.
1030 98. Westermann AJ, Barquist L, Vogel J. 2017. Resolving host-pathogen interactions
1031 by dual RNA-seq. PLoS Pathog 13:e1006033.
1032 99. Arbues A, Lugo-Villarino G, Neyrolles O, Guilhot C, Astarie-Dequeker C. 2014.
1033 Playing hide-and-seek with host macrophages through the use of mycobacterial
1034 cell envelope phthiocerol dimycocerosates and phenolic glycolipids. Front Cell
1035 Infect Microbiol 4:173.
1036 100. Solans L, Uranga S, Aguilo N, Arnal C, Gomez AB, Monzon M, Badiola JJ, Gicquel
1037 B, Martin C. 2014. Hyper-attenuated MTBVAC erp mutant protects against
1038 tuberculosis in mice. Vaccine 32:5192-7.

1039 101. Spertini F, Audran R, Chakour R, Karoui O, Steiner-Monard V, Thierry AC, Mayor
1040 CE, Rettby N, Jaton K, Vallotton L, Lazor-Blanchet C, Doce J, Puentes E, Marinova
1041 D, Aguilo N, Martin C. 2015. Safety of human immunisation with a live-
1042 attenuated Mycobacterium tuberculosis vaccine: a randomised, double-blind,
1043 controlled phase I trial. Lancet Respir Med 3:953-62.
1044 102. Walters SB, Dubnau E, Kolesnikova I, Laval F, Daffe M, Smith I. 2006. The
1045 Mycobacterium tuberculosis PhoPR two-component system regulates genes
1046 essential for virulence and complex lipid biosynthesis. Mol Microbiol 60:312-30.
1047 103. Frigui W, Bottai D, Majlessi L, Monot M, Josselin E, Brodin P, Garnier T, Gicquel B,
1048 Martin C, Leclerc C, Cole ST, Brosch R. 2008. Control of M. tuberculosis ESAT-6
1049 secretion and specific T cell recognition by PhoP. PLoS Pathog 4:e33.
1050 104. Mendoza Lopez P, Golby P, Wooff E, Nunez Garcia J, Garcia Pelayo MC, Conlon K,
1051 Gema Camacho A, Hewinson RG, Polaina J, Suarez Garcia A, Gordon SV. 2010.
1052 Characterization of the transcriptional regulator Rv3124 of Mycobacterium
1053 tuberculosis identifies it as a positive regulator of molybdopterin biosynthesis
1054 and defines the functional consequences of a non-synonymous SNP in the
1055 Mycobacterium bovis BCG orthologue. Microbiology 156:2112-23.
1056 105. Soto CY, Menendez MC, Perez E, Samper S, Gomez AB, Garcia MJ, Martin C.
1057 2004. IS6110 mediates increased transcription of the phoP virulence gene in a
1058 multidrug-resistant clinical isolate responsible for tuberculosis outbreaks. J Clin
1059 Microbiol 42:212-9.

106. Simeone R, Sayes F, Song O, Groschel MI, Brodin P, Brosch R, Majlessi L. 2015. Cytosolic access of Mycobacterium tuberculosis: critical impact of phagosomal acidification control and demonstration of occurrence in vivo. PLoS Pathog 11:e1004650.

107. Burckstummer T, Baumann C, Bluml S, Dixit E, Durnberger G, Jahn H, Planyavsky M, Bilban M, Colinge J, Bennett KL, Superti-Furga G. 2009. An orthogonal proteomic-genomic screen identifies AIM2 as a cytoplasmic DNA sensor for the inflammasome. Nat Immunol 10:266-72.

108. Fernandes-Alnemri T, Yu JW, Datta P, Wu J, Alnemri ES. 2009. AIM2 activates the inflammasome and cell death in response to cytoplasmic DNA. Nature 458:509-13.

109. Unterholzner L, Keating SE, Baran M, Horan KA, Jensen SB, Sharma S, Sirois CM, Jin T, Latz E, Xiao TS, Fitzgerald KA, Paludan SR, Bowie AG. 2010. IFI16 is an innate immune sensor for intracellular DNA. Nat Immunol 11:997-1004.

110. Ishikawa H, Barber GN. 2008. STING is an endoplasmic reticulum adaptor that facilitates innate immune signalling. Nature 455:674-8.

111. Yoneyama M, Kikuchi M, Matsumoto K, Imaizumi T, Miyagishi M, Taira K, Foy E, Loo YM, Gale M, Jr., Akira S, Yonehara S, Kato A, Fujita T. 2005. Shared and unique functions of the DExD/H-box helicases RIG-I, MDA5, and LGP2 in antiviral innate immunity. J Immunol 175:2851-8.

112. Connolly DJ, Bowie AG. 2014. The emerging role of human PYHIN proteins in innate immunity: implications for health and disease. Biochem Pharmacol 92:405-14.

113. Dorhoi A, Nouailles G, Jorg S, Hagens K, Heinemann E, Pradl L, Oberbeck-Muller D, Duque-Correa MA, Reece ST, Ruland J, Brosch R, Tschopp J, Gross O, Kaufmann SH. 2012. Activation of the NLRP3 inflammasome by Mycobacterium tuberculosis is uncoupled from susceptibility to active tuberculosis. Eur J Immunol 42:374-84.

114. Wong KW, Jacobs WR, Jr. 2011. Critical role for NLRP3 in necrotic death triggered by Mycobacterium tuberculosis. Cell Microbiol 13:1371-84.

115. Groschel MI, Sayes F, Shin SJ, Frigui W, Pawlik A, Orgeur M, Canetti R, Honore N, Simeone R, van der Werf TS, Bitter W, Cho SN, Majlessi L, Brosch R. 2017. Recombinant BCG Expressing ESX-1 of Mycobacterium marinum Combines Low Virulence with Cytosolic Immune Signaling and Improved TB Protection. Cell Rep 18:2752-2765.

116. Mishra BB, Moura-Alves P, Sonawane A, Hacohen N, Griffiths G, Moita LF, Anes E. 2010. Mycobacterium tuberculosis protein ESAT-6 is a potent activator of the NLRP3/ASC inflammasome. Cell Microbiol 12:1046-63.

117. Maji A, Misra R, Kumar Mondal A, Kumar D, Bajaj D, Singhal A, Arora G, Bhaduri A, Sajid A, Bhatia S, Singh S, Singh H, Rao V, Dash D, Baby Shalini E, Sarojini Michael J, Chaudhary A, Gokhale RS, Singh Y. 2015. Expression profiling of lymph

nodes in tuberculosis patients reveal inflammatory milieu at site of infection. Sci Rep 5:15214.

118. Casson CN, Yu J, Reyes VM, Taschuk FO, Yadav A, Copenhaver AM, Nguyen HT, Collman RG, Shin S. 2015. Human caspase-4 mediates noncanonical inflammasome activation against gram-negative bacterial pathogens. Proc Natl Acad Sci U S A 112:6688-93.

119. Dutta NK, Illei PB, Jain SK, Karakousis PC. 2014. Characterization of a novel necrotic granuloma model of latent tuberculosis infection and reactivation in mice. Am J Pathol 184:2045-55.

120. Wiens KE, Ernst JD. 2016. The Mechanism for Type I Interferon Induction by Mycobacterium tuberculosis is Bacterial Strain-Dependent. PLoS Pathog 12:e1005809.

121. Bryant CE, Monie TP. 2012. Mice, men and the relatives: cross-species studies underpin innate immunity. Open Biol 2:120015.

122. Brunette RL, Young JM, Whitley DG, Brodsky IE, Malik HS, Stetson DB. 2012. Extensive evolutionary and functional diversity among mammalian AIM2-like receptors. J Exp Med 209:1969-83.

123. Eklund D, Welin A, Andersson H, Verma D, Soderkvist P, Stendahl O, Sarndahl E, Lerm M. 2014. Human gene variants linked to enhanced NLRP3 activity limit intramacrophage growth of Mycobacterium tuberculosis. J Infect Dis 209:749-53.

124. Said-Salim B, Mostowy S, Kristof AS, Behr MA. 2006. Mutations in Mycobacterium tuberculosis Rv0444c, the gene encoding anti-SigK, explain high

1123 level expression of MPB70 and MPB83 in Mycobacterium bovis. Mol Microbiol

1124 62:1251-63.

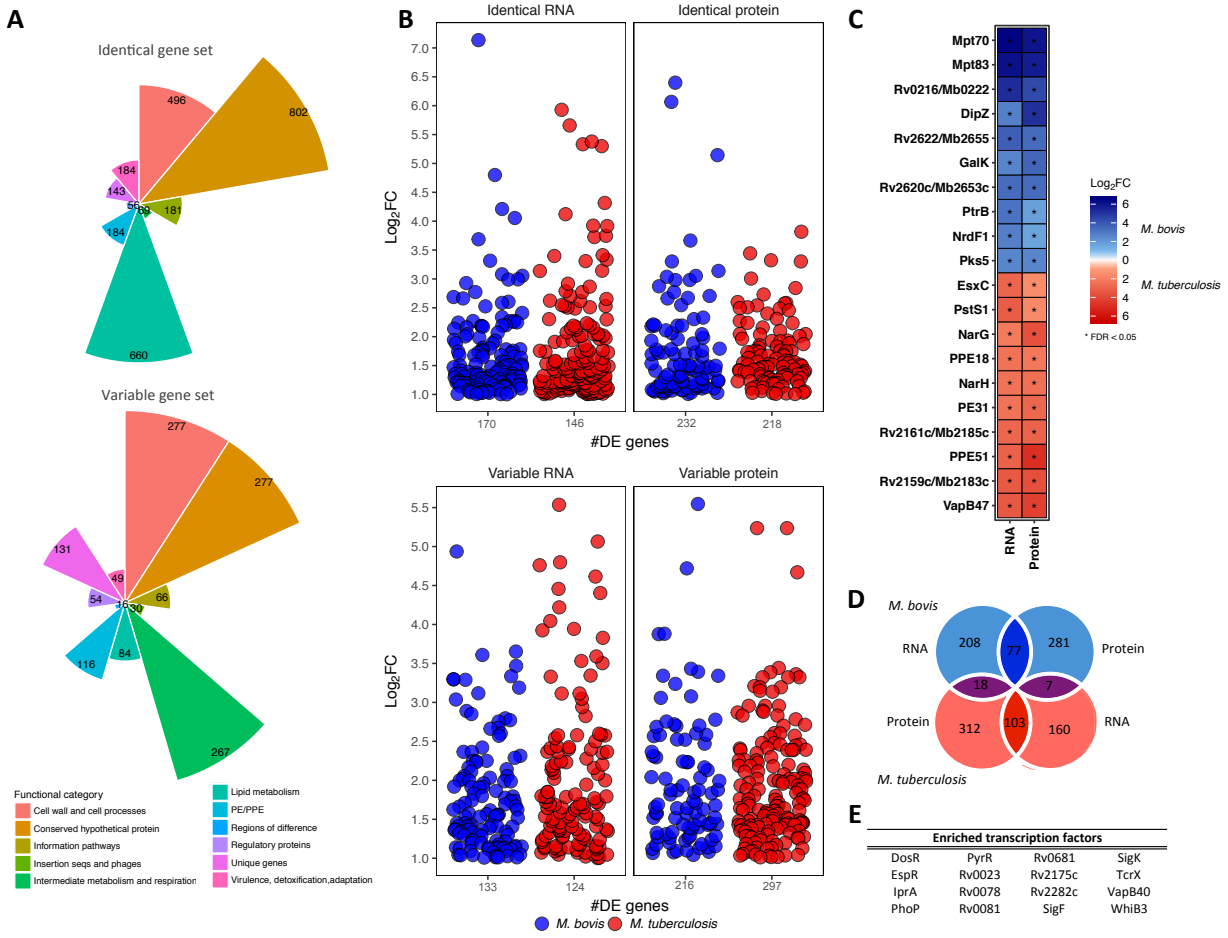

Figure 1: A) The number of genes from *M. bovis* AF2122/97 and *M. tuberculosis* H37Rv classified as either "Identical" (100% conserved in length and amino acid sequence, top plot) or Variable (all other orthologous genes, bottom plot). Colours represent the various gene categories to which each gene belongs. **B)** The level of expression ('Log_2FC') of Identical genes (top panel) and Variable genes (bottom panel) that are differentially expressed ($|Log_2FC| > 1$, FDR < 0.05) and upregulated in either *M. bovis* (blue) or *M. tuberculosis* (red) at both the RNA and protein level. The number of genes in each category is indicated on the x-axis ('#DE genes'). **C)** The top 20 differentially expressed genes at the RNA and protein level ($|Log_2FC| > 1$, FDR < 0.05 ('*')) that are upregulated in *M. bovis* (blue) or *M. tuberculosis* (red). **D)** The overlap of

genes that are upregulated in either *M. bovis* (blue) or *M. tuberculosis* (red) at the RNA and protein level. Dark blue overlap represents those genes upregulated in *M. bovis* only, dark red overlap represents those genes upregulated in *M. tuberculosis* while purple overlaps represent those genes that show discordant expression patterns at the RNA and protein level between the two species. **E)** The transcription factors enriched for Identical genes (100% conserved in length and amino acid sequence between the two species) that are differentially expressed between *M. bovis* and *M. tuberculosis*. (Rand Index, $P < 0.01$).

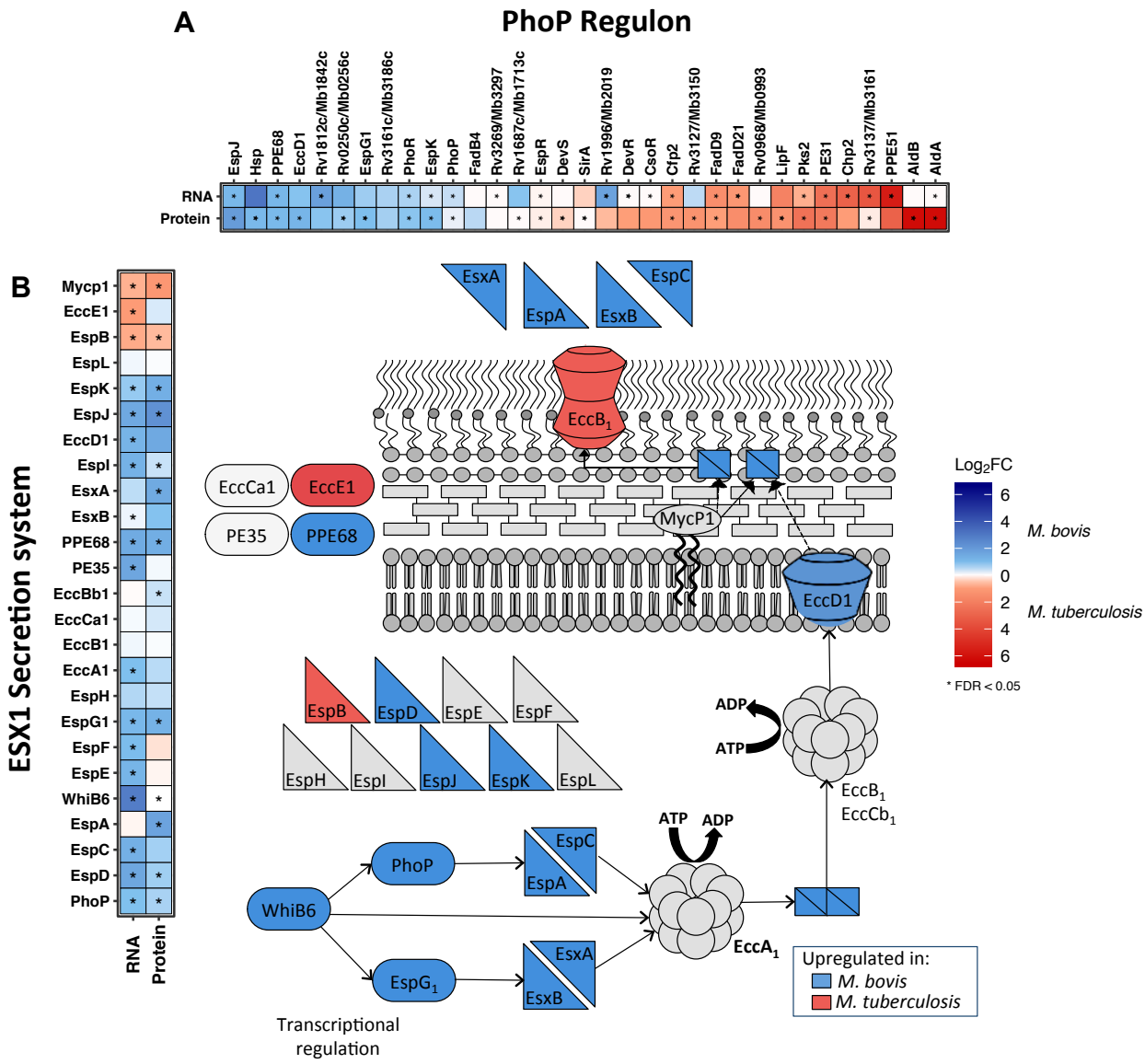

Figure 2: The differentially expressed genes ($|Log_2FC| > 1$, FDR < 0.05 ('*')) belonging to **A)** the PhoP regulon and **B)** the ESX-1 secretion system that are upregulated in *M. bovis* (blue) or *M. tuberculosis* (red). Inset is a representation of the ESX-1 secretion system pathway of *M. tuberculosis* coloured according to the upregulation of the associated gene in *M. bovis* (blue) or *M. tuberculosis* (red).

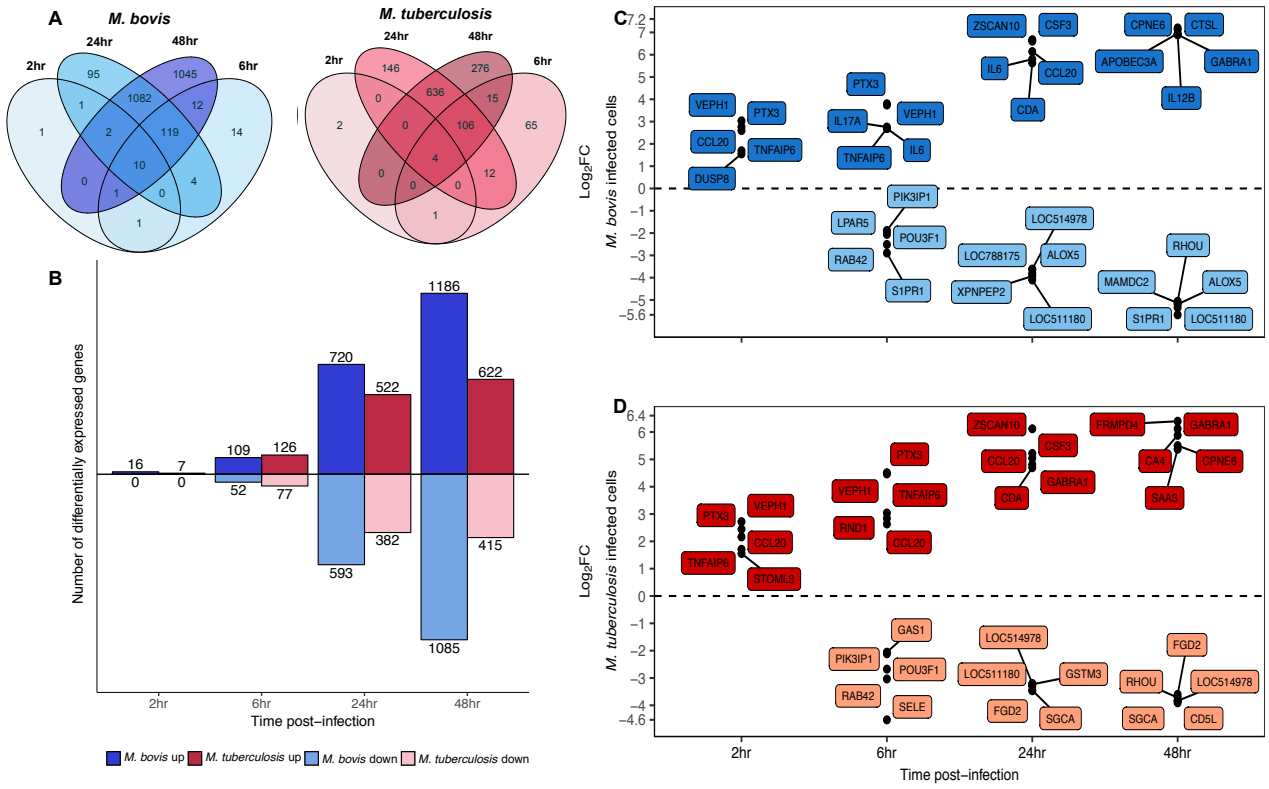

Figure 3: A) The differentially expressed genes (|Log_2FC| > 1, FDR < 0.05) of bovine alveolar macrophages infected with *M. bovis* (blue) or *M. tuberculosis* (red) at 2, 6, 24 and 48 hours post-infection. **B)** The number (y-axis) and direction of change (up = positive y-space, down = negative y-space) of differentially expressed genes (|Log_2FC| > 1, FDR < 0.05) of bovine alveolar macrophages infected with *M. bovis* (blue) or *M. tuberculosis* (red) at 2, 6, 24 and 48 hours post-infection (x-axis). **C)** The top 5 upregulated (positive y-space) and 5 downregulated (negative y-space) differentially expressed genes (|Log_2FC| > 1, FDR < 0.05) of bovine alveolar macrophages infected with *M. bovis* or **D)** *M. tuberculosis* at 2, 6, 24 and 48 hours post-infection (x-axis).

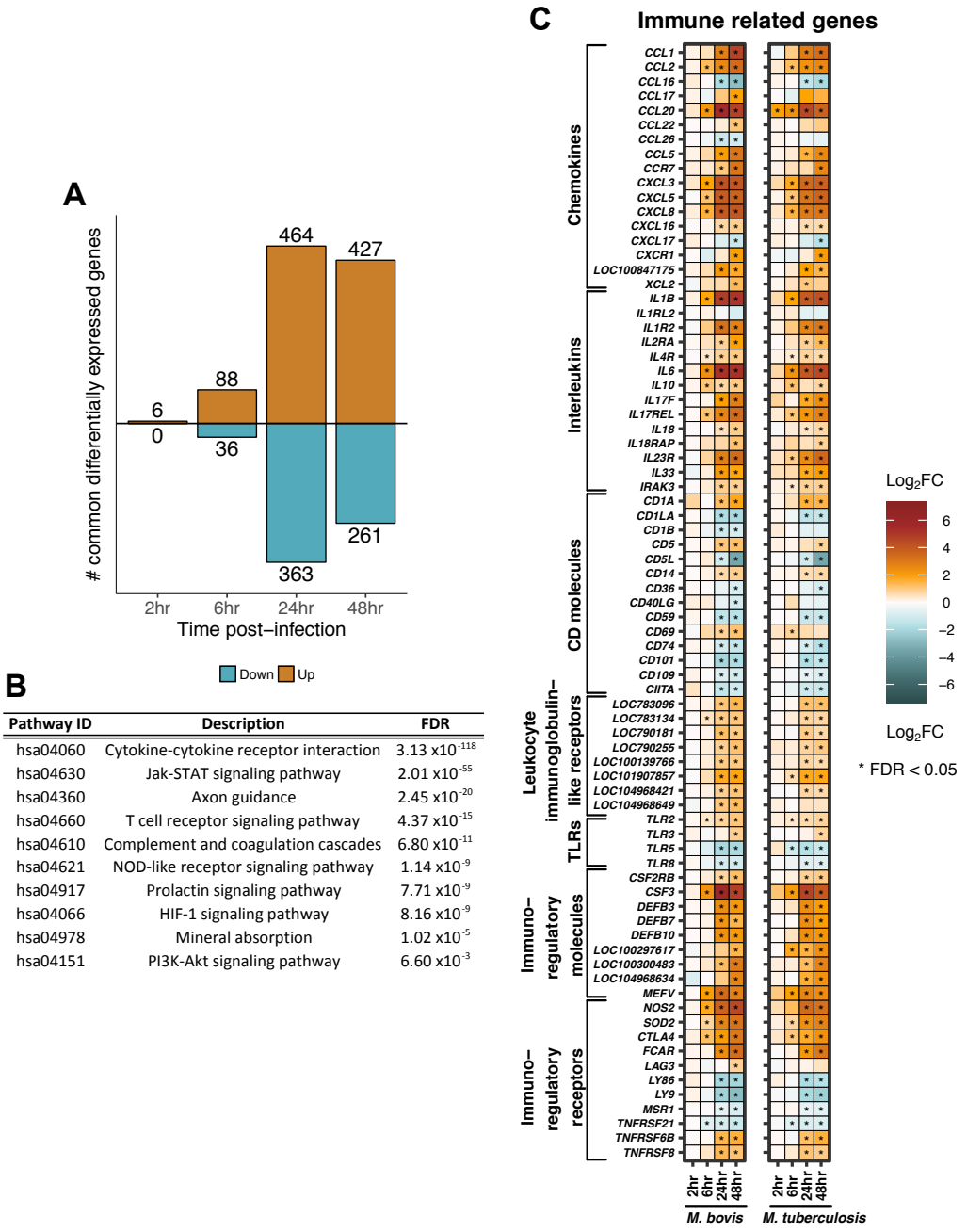

Pathway ID	Description	FDR
hsa04060	Cytokine-cytokine receptor interaction	3.13×10^{-118}
hsa04630	Jak-STAT signaling pathway	2.01×10^{-55}
hsa04360	Axon guidance	2.45×10^{-20}
hsa04660	T cell receptor signaling pathway	4.37×10^{-15}
hsa04610	Complement and coagulation cascades	6.80×10^{-11}
hsa04621	NOD-like receptor signaling pathway	1.14×10^{-9}
hsa04917	Prolactin signaling pathway	7.71×10^{-9}
hsa04066	HIF-1 signaling pathway	8.16×10^{-9}
hsa04978	Mineral absorption	1.02×10^{-5}
hsa04151	PI3K-Akt signaling pathway	6.60×10^{-3}

Figure 4: A) The number (y-axis) and direction of change (up = orange, down = cyan) of genes that are commonly differentially expressed ("core response") ($|\text{Log}_2\text{FC}| > 1$, FDR < 0.05, with non-significant delta comparison values) in bovine alveolar macrophages infected with *M. bovis* and infected with *M. tuberculosis* at 2, 6, 24 and 48 hours post-infection. **B)** Pathways enriched for 688 genes that are commonly differentially expressed ("core response") in bovine alveolar

macrophages infected with *M. bovis* and *M. tuberculosis* over the first 24 hours of infection (FDR < 0.05). **C)** Genes that are commonly differentially expressed ("core response") ($|Log_2FC| > 1$, FDR < 0.05 ('*')) and associated with the innate immune response in bovine alveolar macrophages infected with *M. bovis* (left column) or *M. tuberculosis* (right column) over 48 hours post-infection.

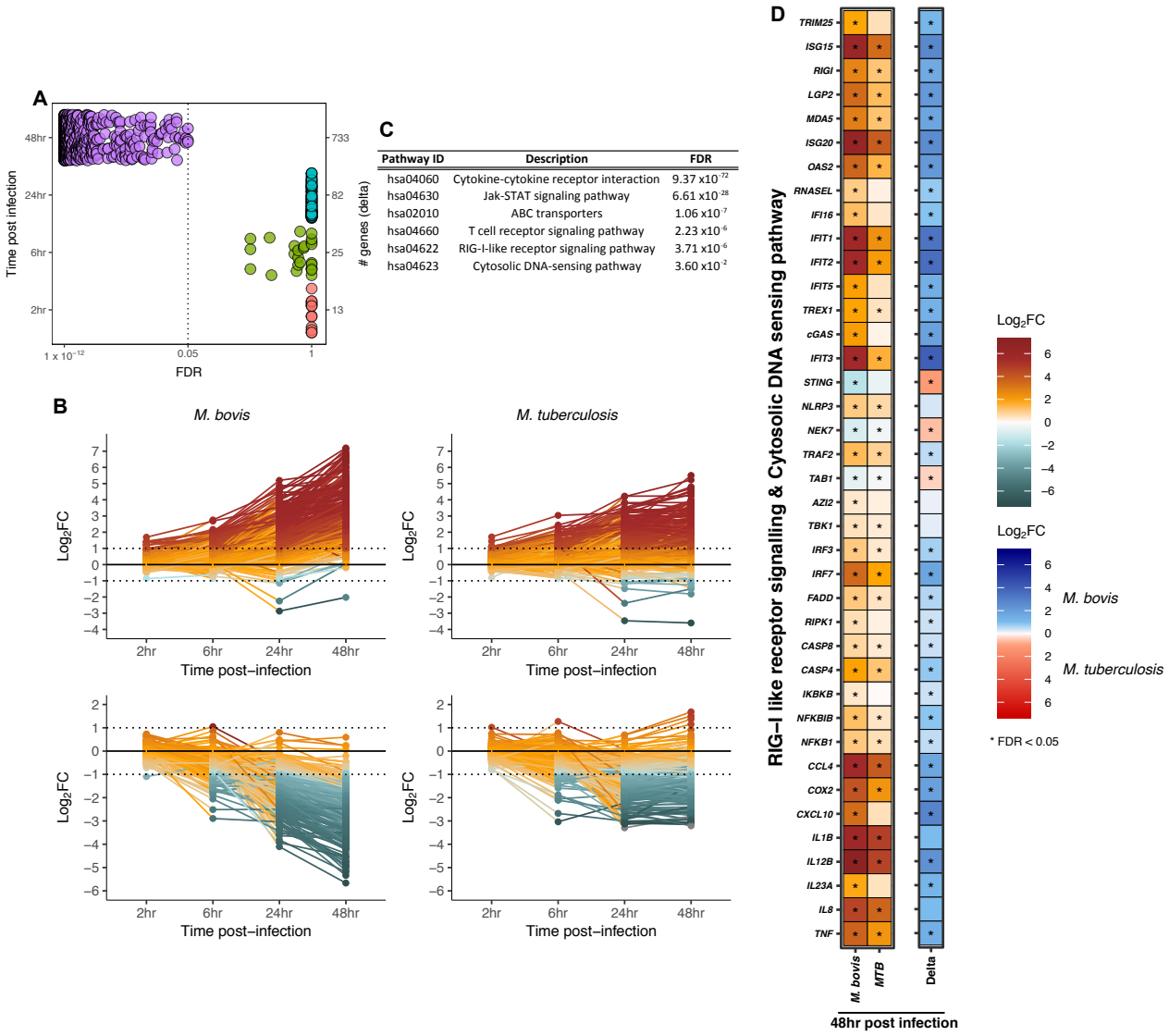

Figure 5: A) The number of genes (right y-axis) that are changing (|Log_2FC| > 1) and that pass FDR threshold (FDR< 0.05) from the comparative analysis of *M. bovis*- or *M. tuberculosis*-infected macrophages in contrast to control macrophages and subsequently in contrast to the other infection series (delta comparison) at 2, 6, 24 and 48 hours post-infection ('# genes (delta)') **B)** Line graphs represent those differentially expressed functionally annotated genes (*n* = 576) that exhibit a higher magnitude of change in *M. bovis*-infected macrophages versus *M. tuberculosis*-infected macrophages in a positive manner (*n* = 323) (left and right top panel

respectively) and in a negative manner (*n* = 253) (left and right bottom panel respectively) at 2, 4, 24 and 48 hours post-infection. **C)** Pathways that are enriched for 576 functionally annotated genes that exhibit divergent expression patterns in *M. bovis*- or *M. tuberculosis*-infected macrophages at 48 hours post-infection (FDR < 0.05). **D)** The differentially expressed genes ($|Log_2FC| > 1$, FDR < 0.05) associated with *RIG-I*-like and *DNA sensing signalling* pathways in bovine alveolar macrophages infected with *M. bovis* (blue) or *M. tuberculosis* (red) at 48 hours post-infection.

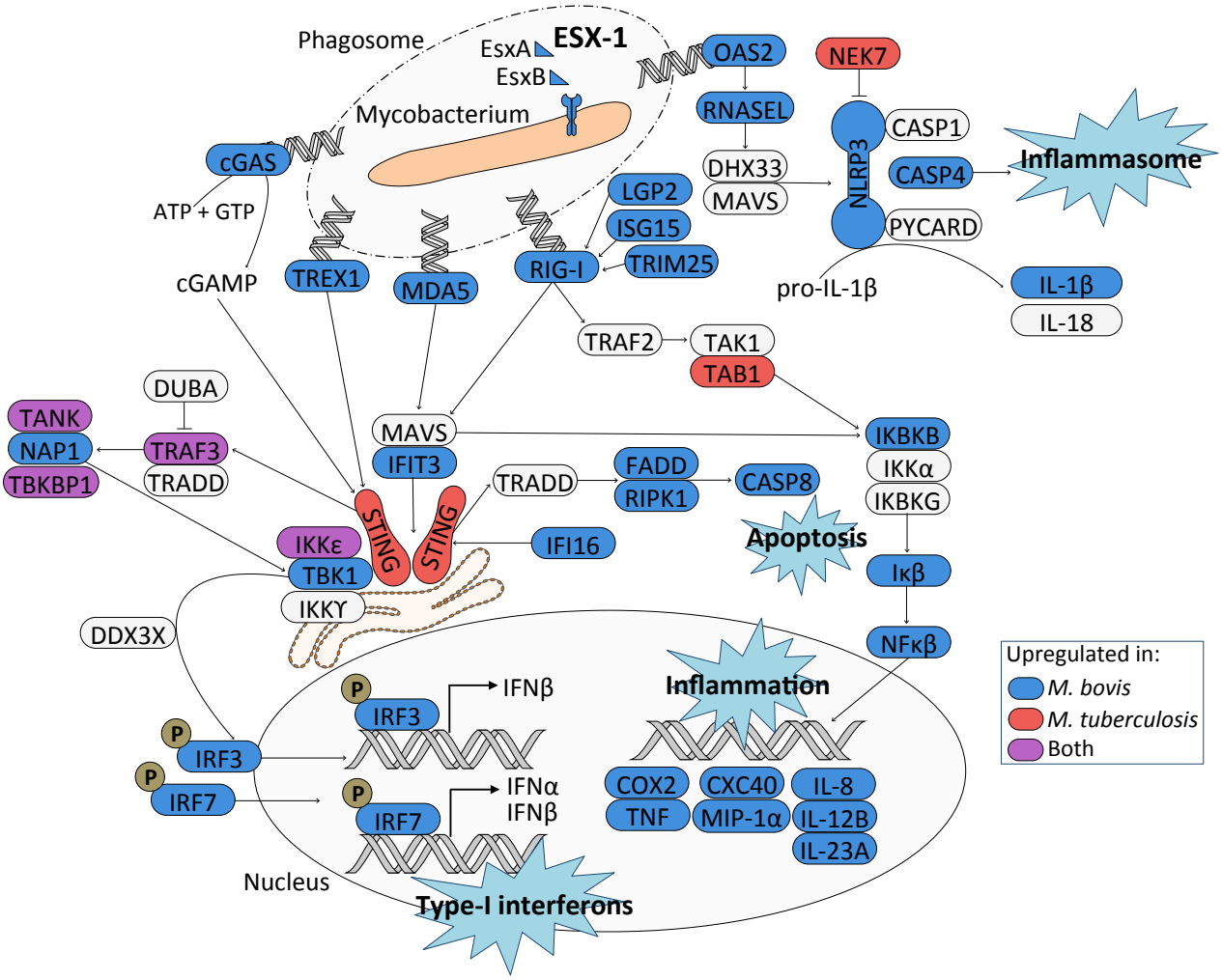

Figure 6: An overview of the DNA sensing and RIG-I signalling identified in this study 48 hours after infection of bovine alveolar macrophages with *M. bovis* and *M. tuberculosis.* Blue and red represents upregulation of the associated gene in either *M. bovis*- or *M. tuberculosis*-infected macrophages while purple represents upregulation of the associated gene in both infection models. The ESX-1 secretion system was found upregulated in *M. bovis* in comparison to *M. tuberculosis*.

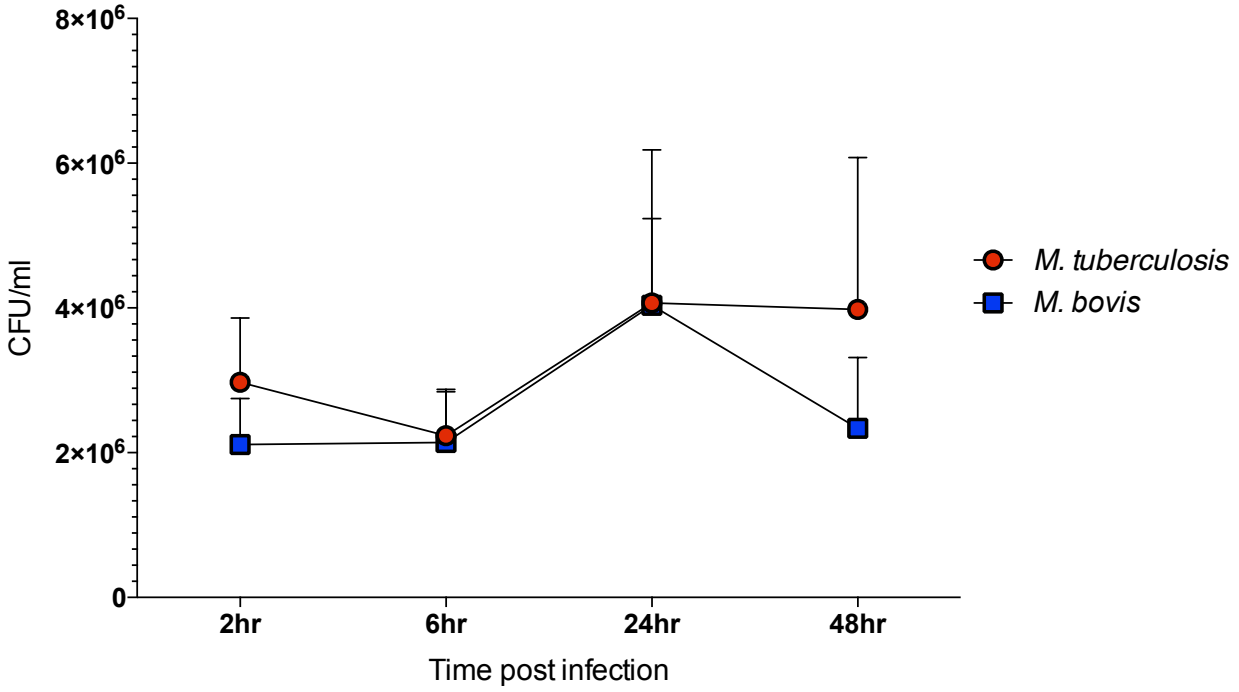

Figure S1: The number of colony forming units ('CFU/ml') recovered from bovine alveolar macrophages infected with *M. bovis* (blue) or *M. tuberculosis* (red) at 2, 6, 24 and 48 hours post-infection. (Error bars represent standard error of the mean, *n* = 6)

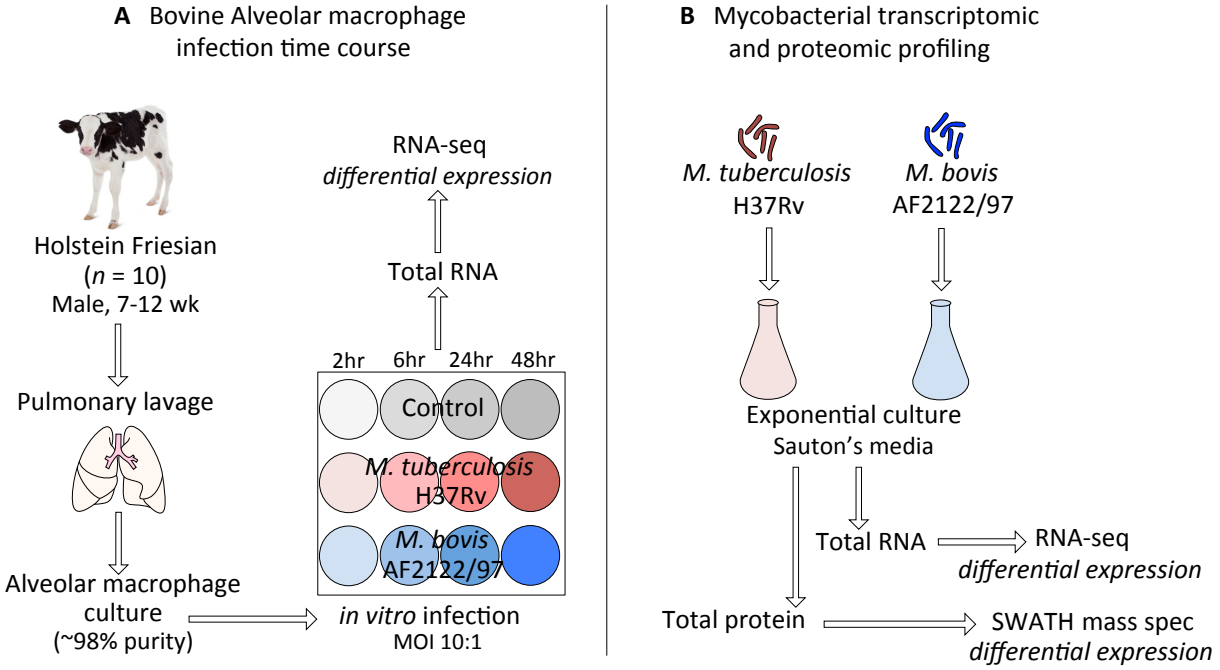

Figure S2: Overview of experimental design for the **A)** bovine alveolar macrophage infection time course and **B)** mycobacterial transcriptomic and proteomic profiling performed for this study.

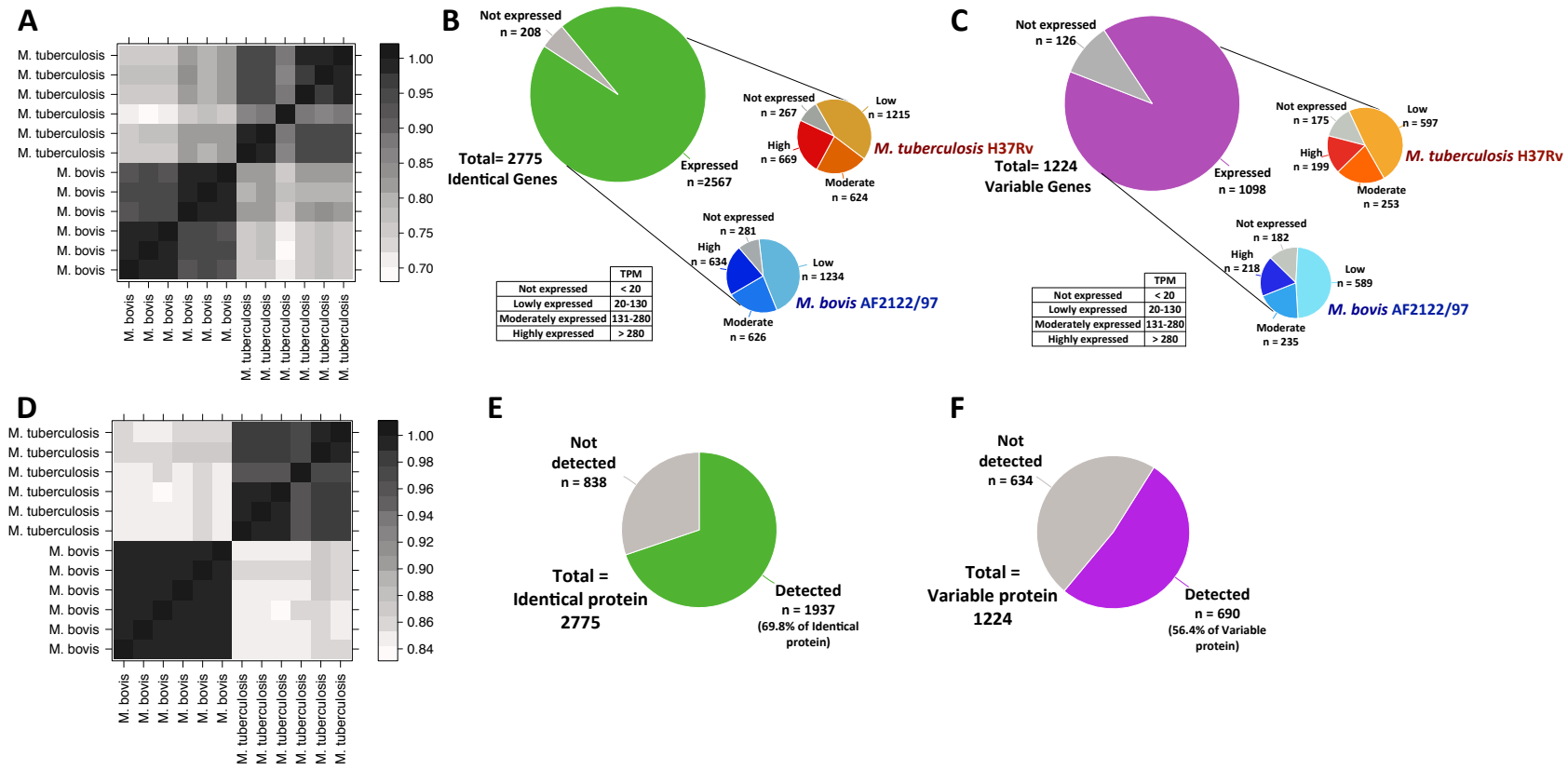

Figure S3: A) Pearson correlation plot of reads mapped to 2,775 Identical genes (100% conserved in length and amino acid sequence between the two species) in the six *M. bovis* and six *M. tuberculosis* RNA-seq datasets. Pie charts representing the proportion of **B)** Identical (100% conserved in length and amino acid sequence between the two species, green) and **C)** Variable genes (< 100% conserved in length and amino acid sequence between the two species, purple) detected and not detected across *M. bovis* and *M. tuberculosis* RNA-seq datasets. RNA expression values (Transcripts per Million (TPM)) were calculated for each gene and gene

expression within either species was categorised into not expressed (<20 TPM), lowly expressed (20-130 TPM), moderately expressed (131-280 TPM) and highly expressed (>280 TPM). **D)** Pearson correlation plot of the intensity values of the 2,627 identified proteins in the six *M. bovis* and six *M. tuberculosis* SWATH MS datasets. Pie charts representing the expression of **E)** 2775 Identical genes (100% conserved in length and amino acid sequence) and **F) 1**224 Variable genes (< 100% conserved in length and amino acid) in *M. bovis* and *M. tuberculosis* detected by SWATH MS.

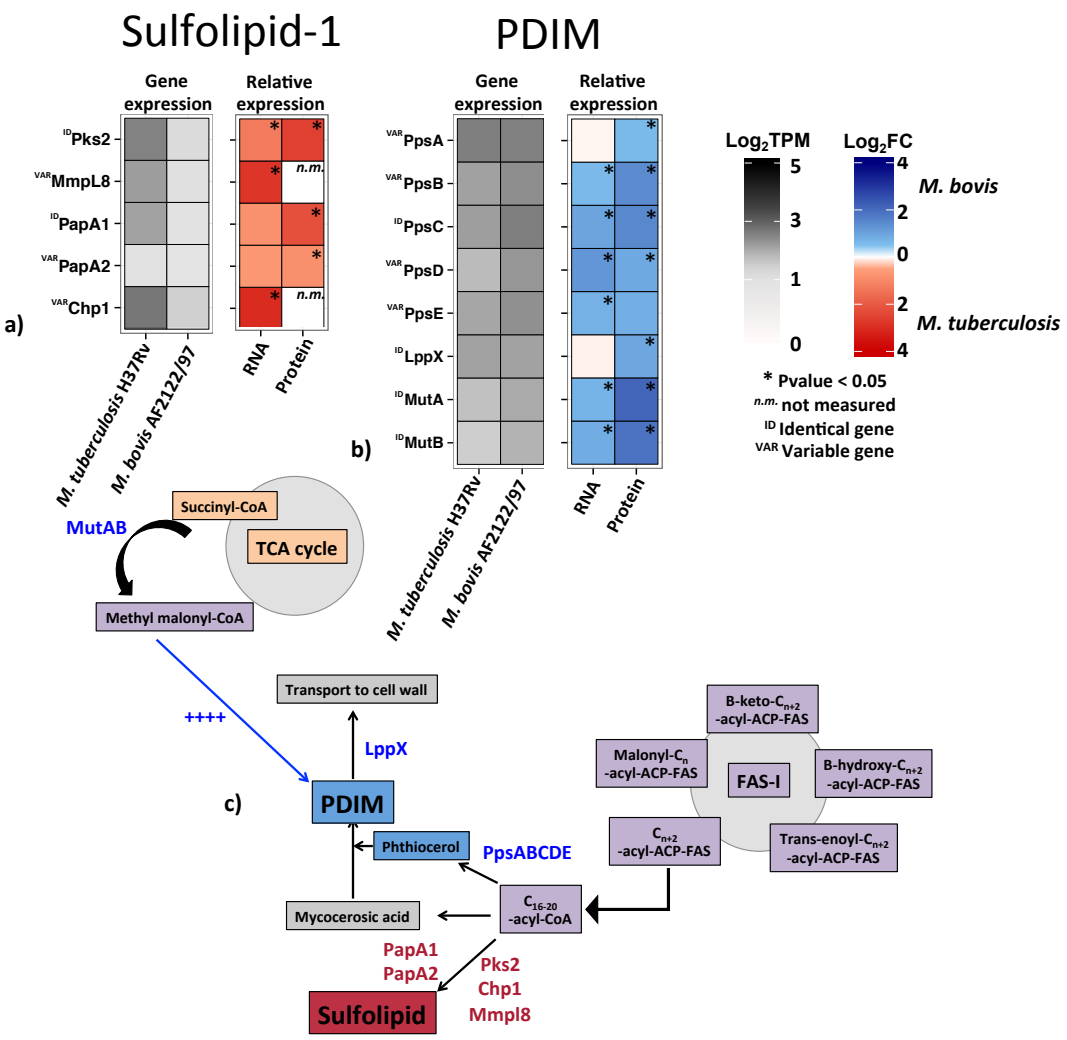

Figure S4: The expression of the **a)** sulfolipid-1 (SL-1) and **b)** phthiocerol dimycocerosate (PDIM) synthesis associated genes at the RNA and protein level in *M. tuberculosis* (red) and *M. bovis* (blue). The expression of each gene ("Gene expression") is presented as Log_{10}TPM at the RNA level while the relative expression ("Relative expression") between the two species is presented as log2FC. Those genes that change significantly at the RNA and protein level (FDR < 0.05) are denoted ('*'). **c)** Diagrammatic overview of the SL-1 and PDIM biosynthesis pathways in *M. tuberculosis*. Blue represents the genes in b) that are upregulated in *M. bovis* in contrast to *M. tuberculosis* and red represents the genes in a) that are upregulated in *M. tuberculosis.*

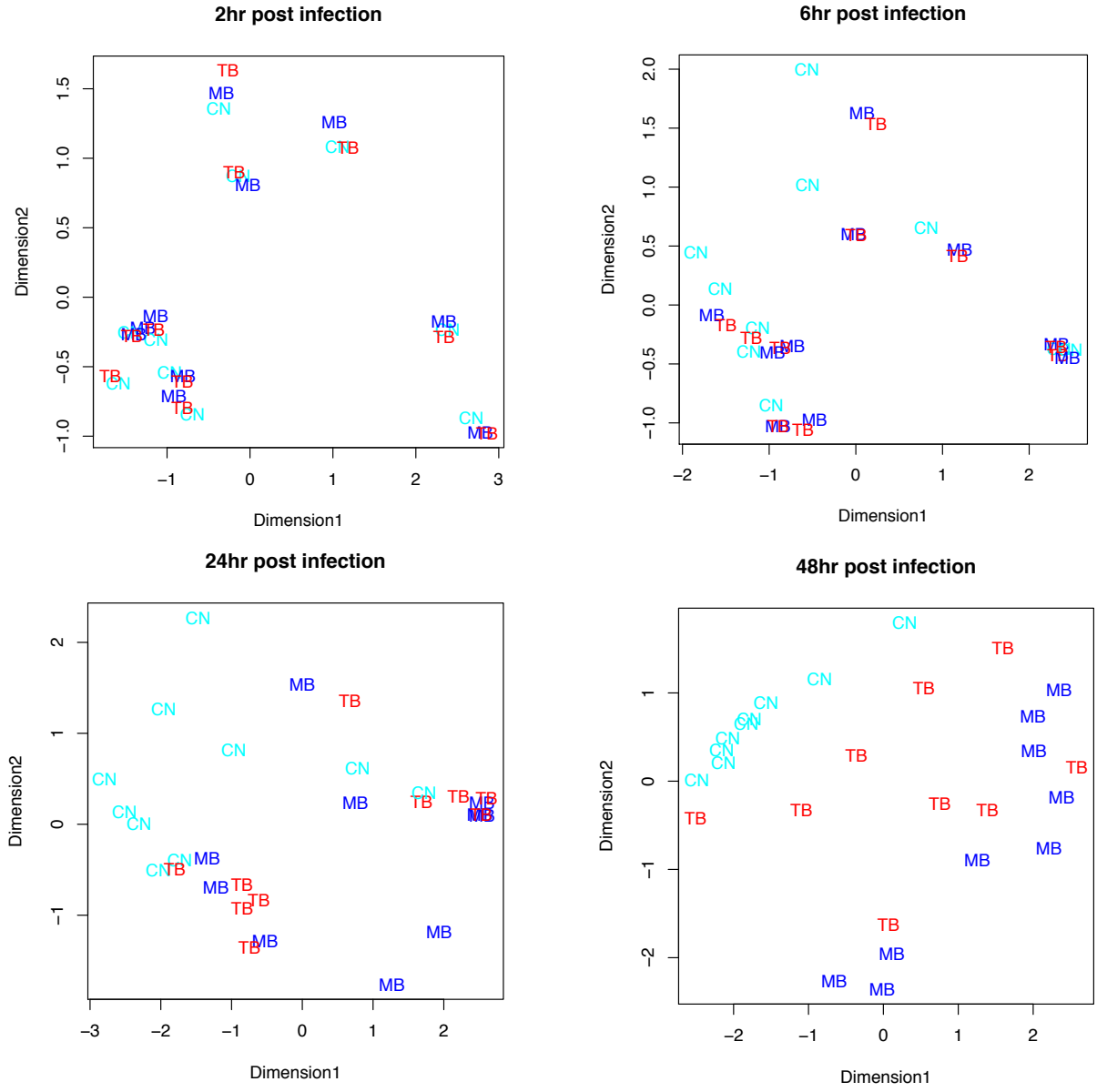

Figure S5: Multidimensional scaling plots of the RNA-seq expression data for individual of bovine alveolar macrophages infected with *M. bovis* ('MB', blue), *M. tuberculosis* ('TB', red) or none ('CN', cyan) at 2, 6, 24 ad 48 hours post-infection.

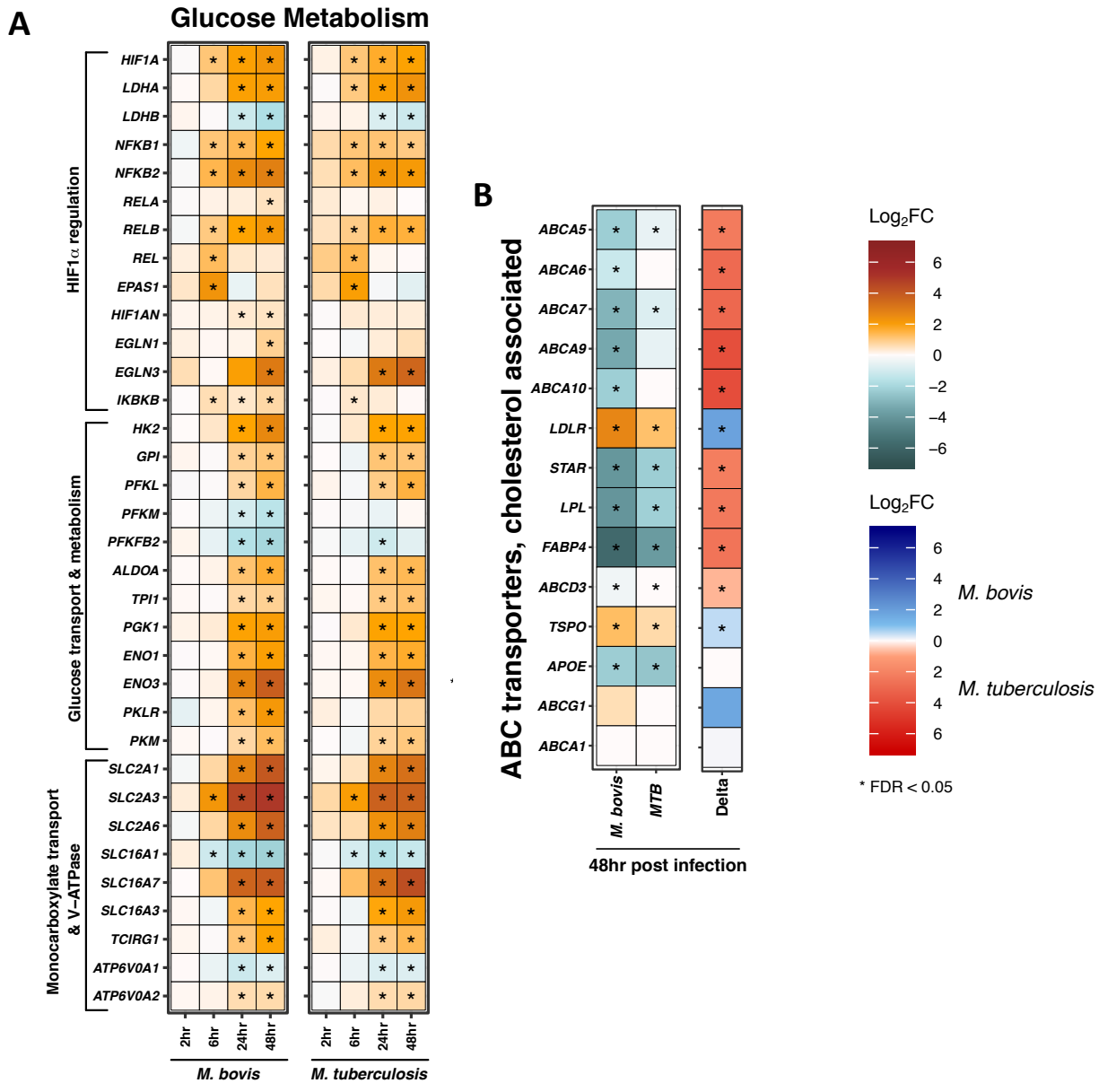

Figure S6: The expression of differentially expressed genes ($|Log_2FC| > 1$, FDR < 0.05 ('*') associated with **A)** glucose metabolism in bovine alveolar macrophages infected with *M. bovis* or *M. tuberculosis* ("MTB") at 2, 6, 24 and 48 hours post-infection and **B)** cholesterol-associated transport in bovine alveolar macrophages at 48 hours post-infection. Delta comparison shows genes upregulated in *M. bovis* in blue and *M. tuberculosis* in red.